# Time-dependent Monte Carlo Simulation

Umberto Ravaioli

Beckman Institute and
Department of Electrical and Computer Engineering
University of Illinois at Urbana-Champaign
Urbana, IL 61801, USA

## Monte Carlo simulation is time-dependent

- but to obtain true time-dependent results, the transients need to be resolved self-consistently.
- Noise is a difficult issue. Often, techniques to reduce noise apply averaging in a way that assumes steady-state, making the transient not physical.
- In steady-state simulation, we usually apply bias assuming ideal voltage sources. This eliminates the displacement current. In a transient simulation where the external circuit is present, displacement current must also be included.
- Is the electrostatic Poisson equation sufficient to describe a transient situation?

# 1-D simulation

- Consider a 1-D structure of length $L$, cross-sectional area $A_o$ and applied bias $V_D$. The displacement current may be averaged and lumped in a single circuit parameter (we consider only electron current for simplicity)

$$\underbrace{I(t)}_{\substack{\text{total}\\ \text{current}}} = \underbrace{I_e(x,t)}_{\substack{\text{electron}\\ \text{current}}} + \underbrace{\varepsilon A_o \frac{\partial E(x,t)}{\partial t}}_{\substack{\text{displacement}\\ \text{current}}}$$

$$I(t) = \frac{1}{L}\int_0^L \left( I_e(x,t) + \varepsilon A_o \frac{\partial E(x,t)}{\partial t} \right) dx =$$

$$= \frac{1}{L}\int_0^L I_e(x,t)\, dx + \frac{\varepsilon A_o}{L}\frac{\partial V_D}{\partial t}$$

# Cold Capacitance

- The term

$$\frac{\varepsilon A_o}{L}\frac{\partial V_D}{\partial t}$$

contains all the information about the displacement current. It can be represented by an external capacitance, included in the circuit connected to the device.

$$\frac{\varepsilon A_o}{L} = C_c = \text{cold capacitance}$$

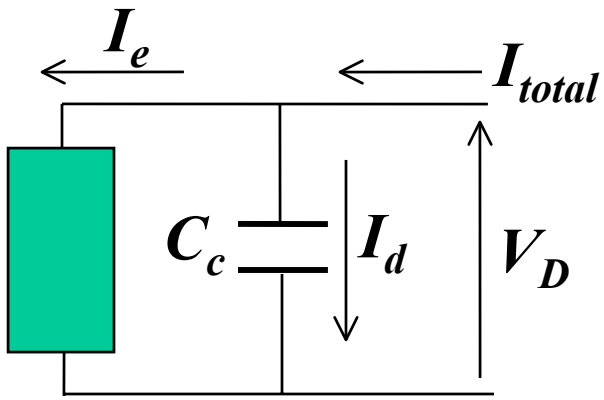

# Example: Gunn diode circuit

- **The non-linear part of the diode is simulated by using Monte Carlo (3-valleys non-parabolic model). Displacement current is accounted for by a time-dependent voltage boundary condition at the terminals of the cold capacitance.**

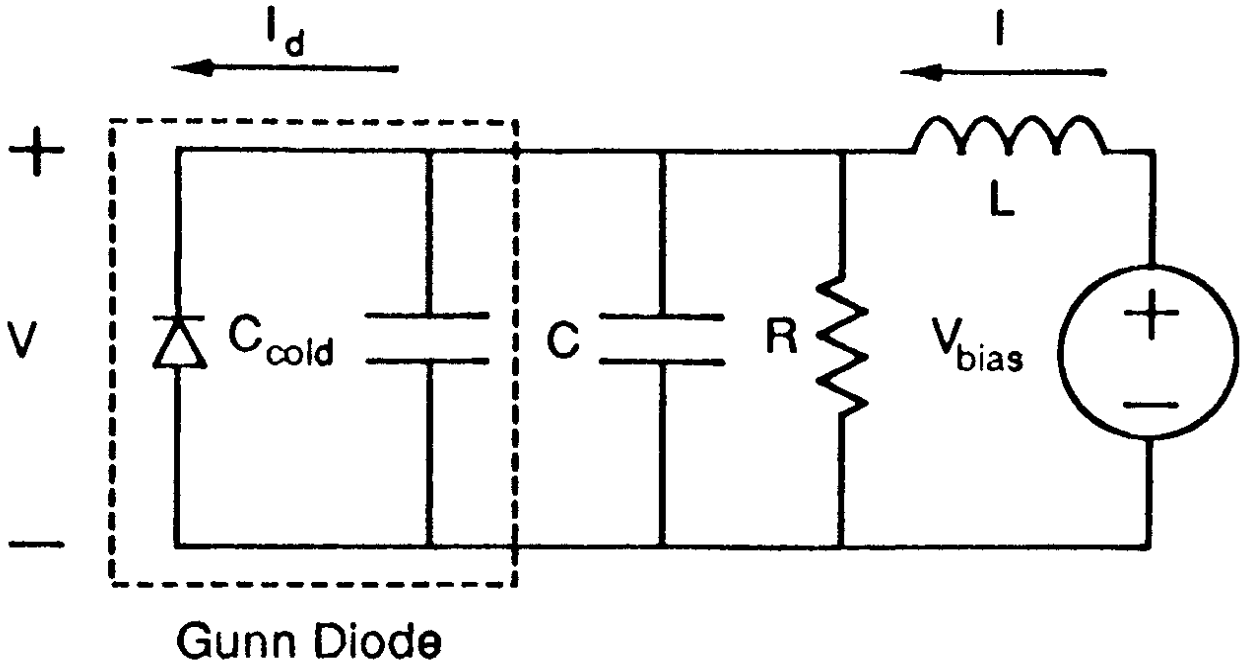

# External circuit equations

- **Kirchhoff's equations**

$$V_D(t) = V_B - L\frac{d\,I(t)}{d\,t}$$

$$I(t) = I_d(t) + C_{tot}\frac{d\,V_D(t)}{d\,t} + \frac{V_D}{R} \qquad C_{tot} = C + C_{cold}$$

- **Finite difference discretization in time**

$$I(t+\Delta t) = \left[V_B - V_D(t)\right]\frac{\Delta t}{L} + I\left(t\right)$$

$$V_D(t+\Delta t) = \left[I(t) - I_d(t)\right]\frac{\Delta t}{C_{tot}} + V_D(t)\left[1 - \frac{\Delta t}{R\,C}\right]$$

# Gunn diode test structures

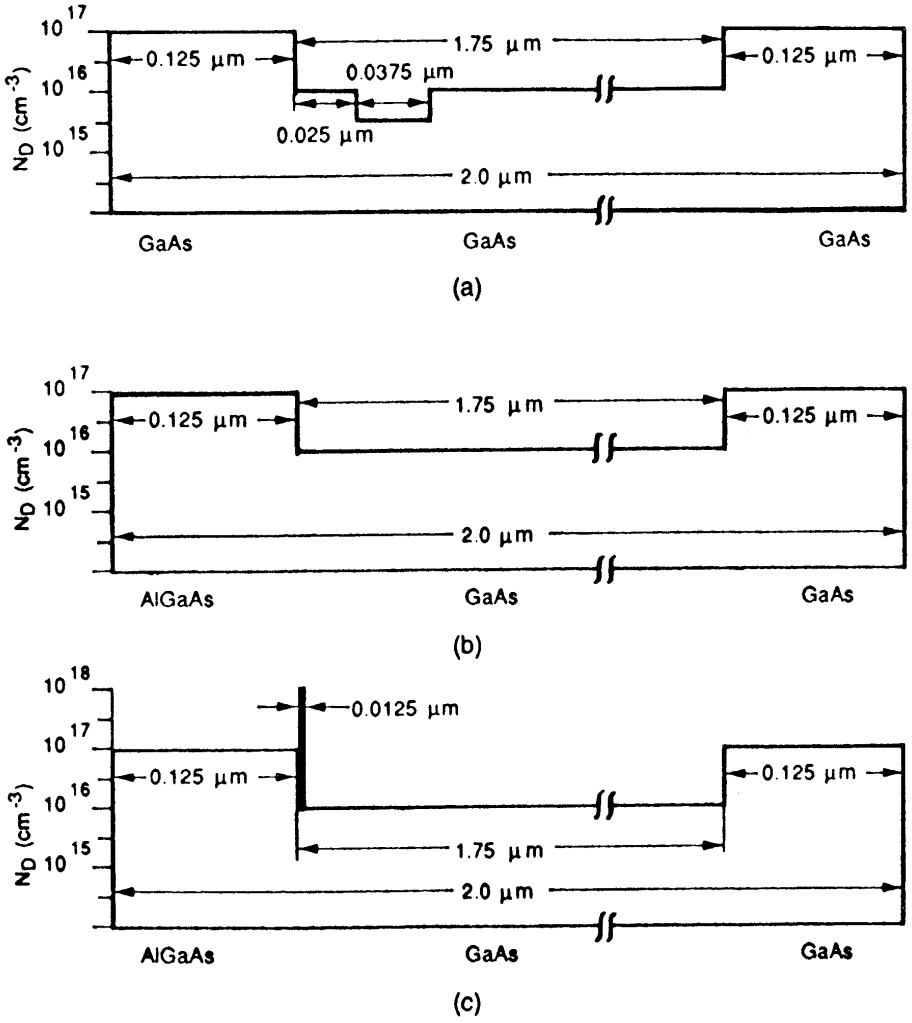


**Homojunction**

**"Notch" oscillator**

**Heterojunction**

**Heterojunction**

**+ doping spike**

# Band structure valleys in GaAs and AlGaAs

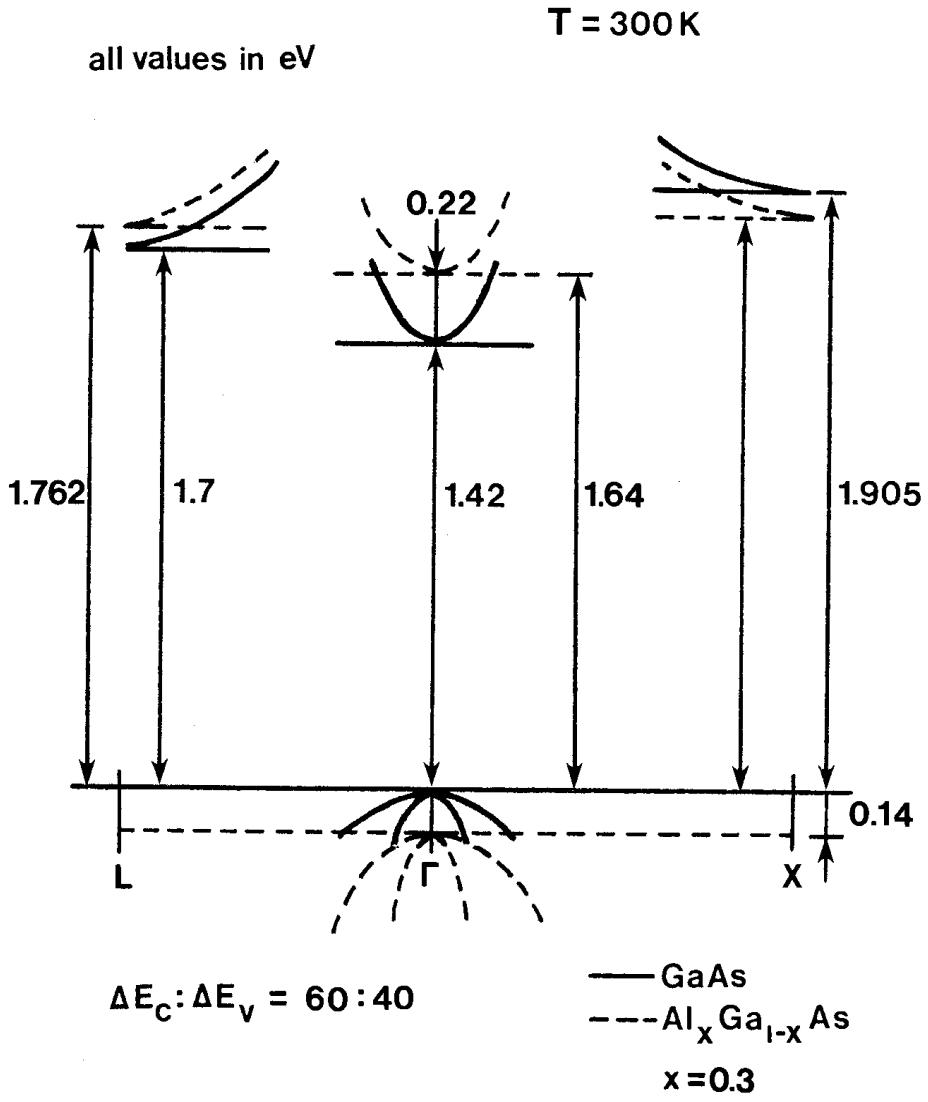

# Structure 1: accumulation domain cycle

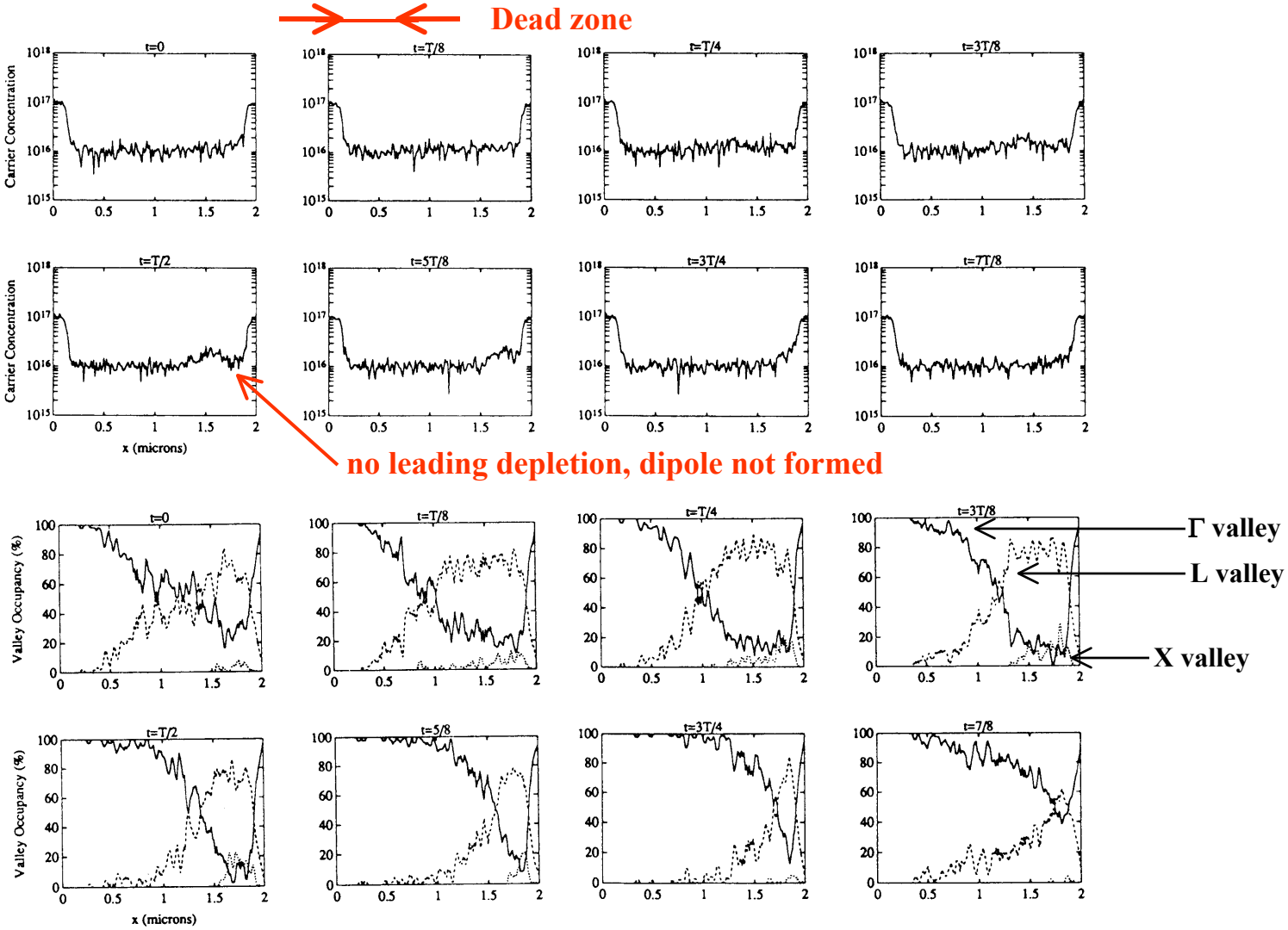

# Structure 2: well-formed domain cycle

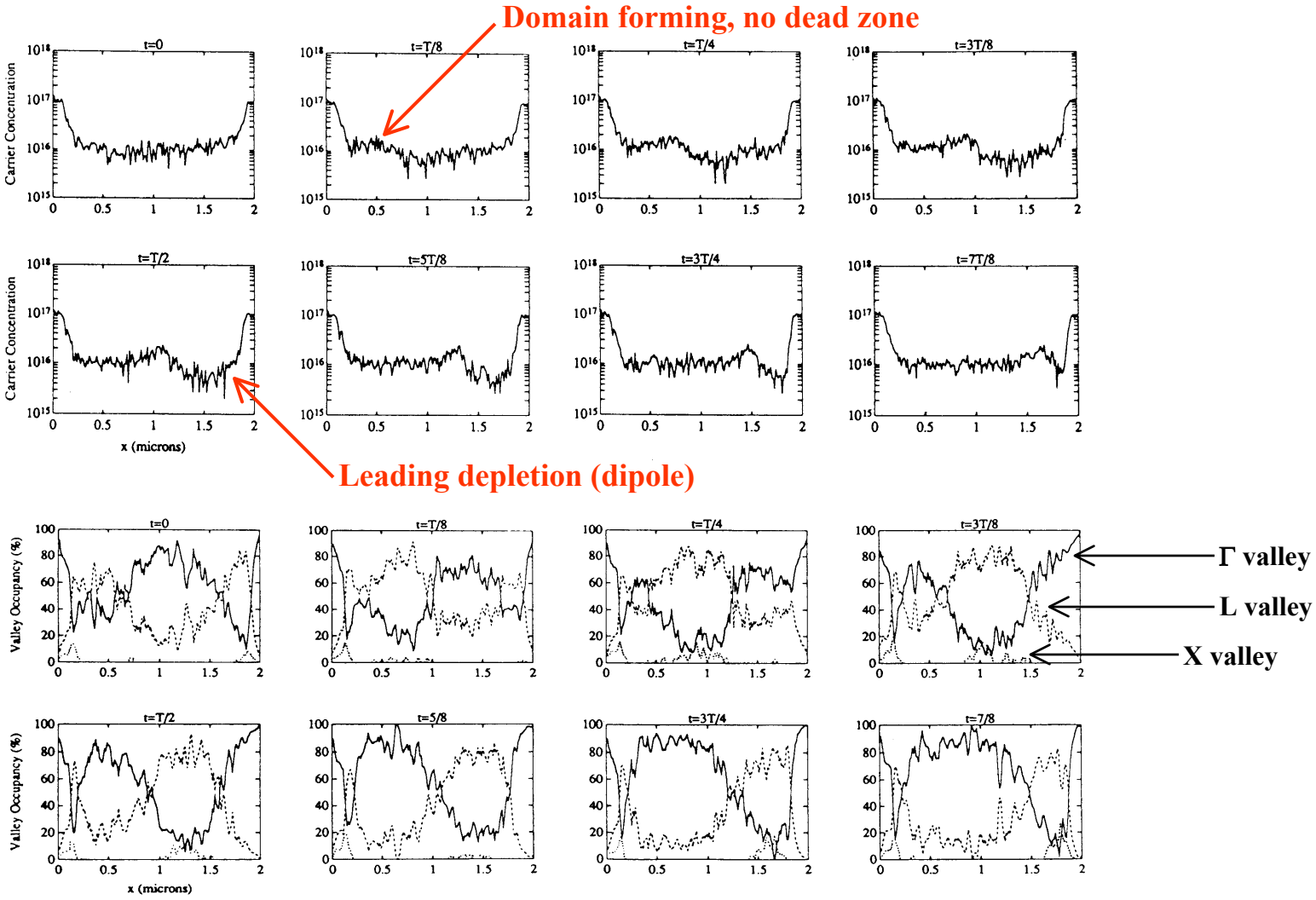

# Electric potential evolution - comparison

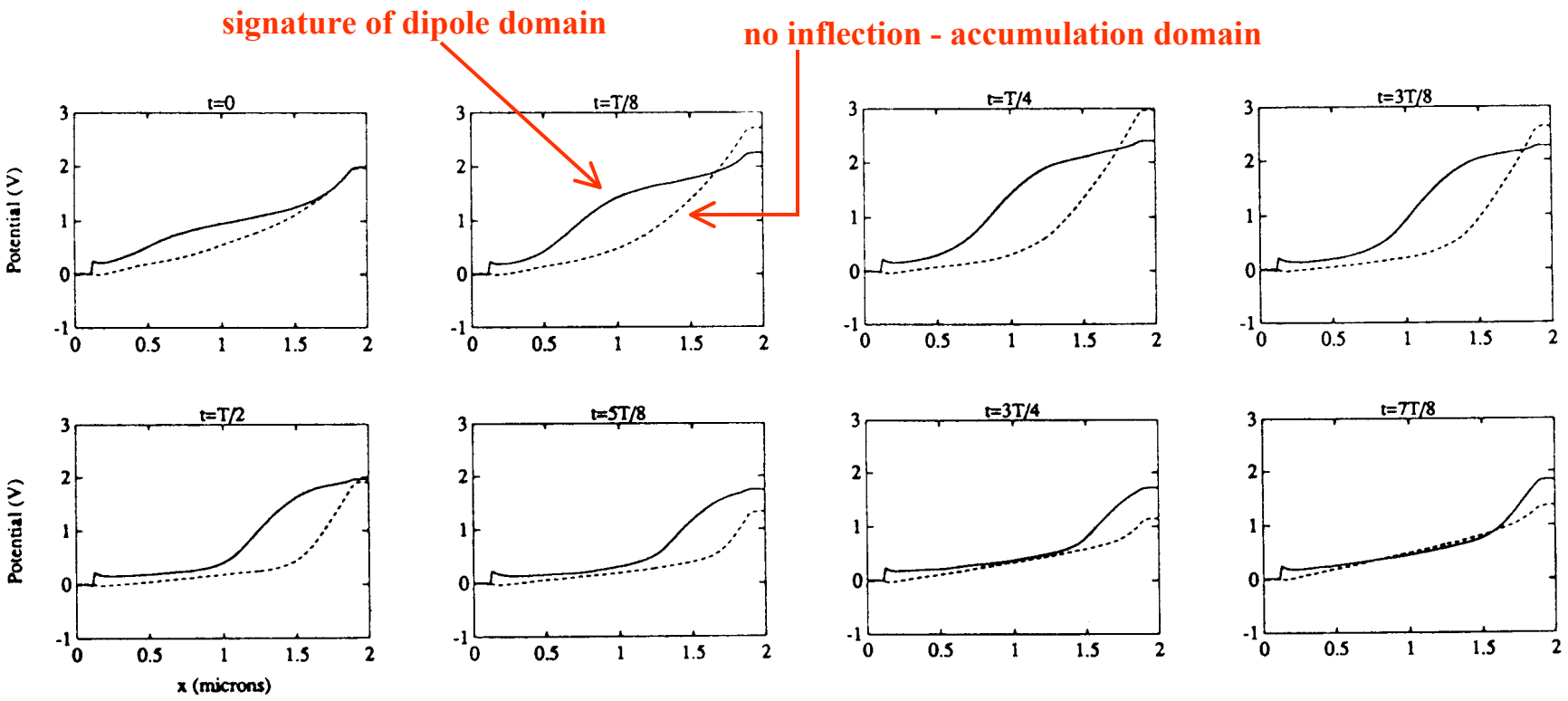


--------- Notch oscillator - accumulation domain

———— Hetrojunction cathode oscillator - well-formed domain

# Structure 3: accumulation domain cycle, again

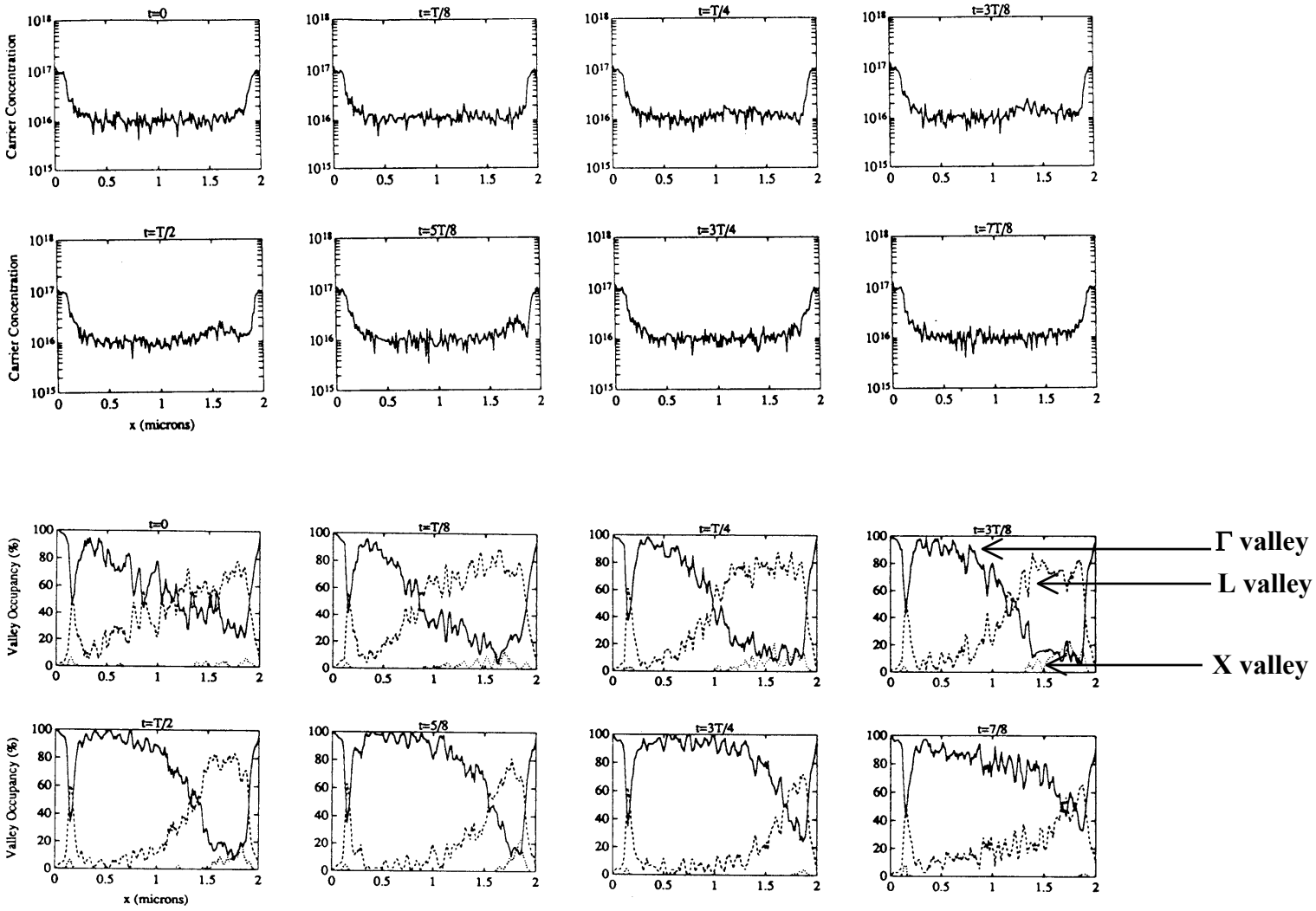

# Comparative Results

TABLE I
RF PERFORMANCE OF THE GUNN OSCILLATORS

| Type | $V_B$ (V) | f (GHz) | $P_s$ (mW) | $P_d$ (mW) | $P_{ac}$ (mW) | $\eta$ (%) | $x$ |
|---|---|---|---|---|---|---|---|
| Notch | 1.5 | 92.06 | 511.09 | 412.09 | 9.00 | 1.76 | 0.00 |
| | 2.0 | 94.69 | 716.28 | 538.60 | 17.67 | 2.47 | 0.00 |
| | 2.5 | 95.43 | 938.40 | 664.41 | 23.99 | 2.56 | 0.00 |
| HC1 | 1.5 | 80.98 | 416.26 | 324.72 | 1.54 | 0.37 | 0.33 |
| | 2.0 | 85.67 | 597.42 | 434.34 | 3.09 | 0.52 | 0.33 |
| HC2 | 1.5 | 92.40 | 506.26 | 408.28 | 7.98 | 1.58 | 0.23 |
| | 2.0 | 94.27 | 700.32 | 523.12 | 17.20 | 2.46 | 0.23 |
| | 2.5 | 95.08 | 924.70 | 651.25 | 23.45 | 2.54 | 0.23 |
| HCS | 1.5 | 92.85 | 509.21 | 410.01 | 9.20 | 1.81 | 0.23 |
| | 2.0 | 95.36 | 715.36 | 537.53 | 17.83 | 2.49 | 0.23 |
| | 2.5 | 95.58 | 932.02 | 659.15 | 22.88 | 2.46 | 0.23 |

$V_B$ is the dc bias voltage, $f$ is the frequency of the signal current obtained from the simulations, $P_s$ is the time-averaged power supplied by the battery to the circuit, $P_d$ is the total power dissipated in the device (ac and dc), $P_{ac}$ is the ac power delivered to the load resistor, $\eta$ is the efficiency, defined as the ratio between the ac power delivered to the load and the time-averaged power supplied by the battery, and $x$ is the Al mole fraction. The natural frequency of the RLC network (including the cold capacitance) is 104.95 GHz.

# Multi-dimensional device

- Current through a contact over a time-step $\Delta t$

$$I(t) = \frac{qZ}{z\,\Delta t}\Big( \underbrace{\Delta N_a}_{\substack{particles\\ absorbed\\ in\ \Delta t}} - \underbrace{\Delta N_i}_{\substack{particles\\ injected\\ in\ \Delta t}} \Big) + \underbrace{\varepsilon_s \varepsilon_0 Z \int \frac{d E_\perp}{d t} dx}_{\substack{displacement\ current\\ \int\ over\ contact\ length}}$$

$Z$ = actual lateral width of device

$z$ = simulated lateral width

$$Q(t) = \underbrace{\frac{q Z}{z}(N_a - N_i) + \varepsilon_s \varepsilon_0 Z \int E_\perp(x,t)\,dx}_{\substack{cumulative\ terminal\ charge\\ (N_a, N_i\ \text{integrated up to time}\ t)}}$$

(Hockney and Eastwood, 1981)

- **Example: GaAs MESFET** **(Patil and Ravaioli, Solid-State Electronics,1991)**

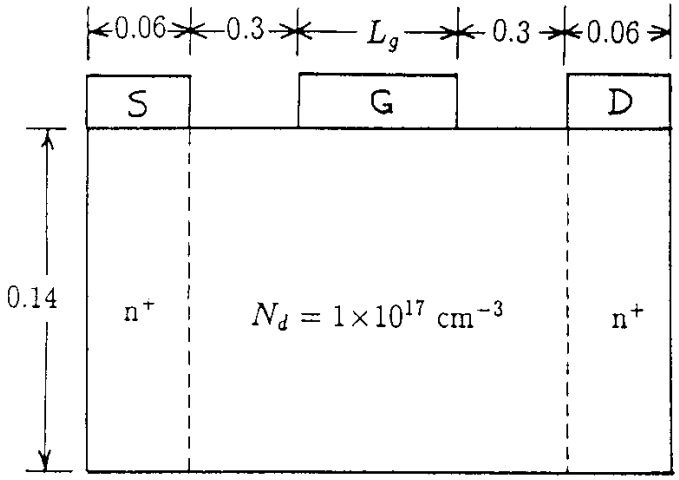


Fig. 1. MESFET structure used in this simulation. All dimensions are in micron. The doping density in the source/drain region is $3 \times 10^{17}\,\mathrm{cm}^{-3}$. The gate length $L_g$ is 0.3 or 0.5 $\mu$m.

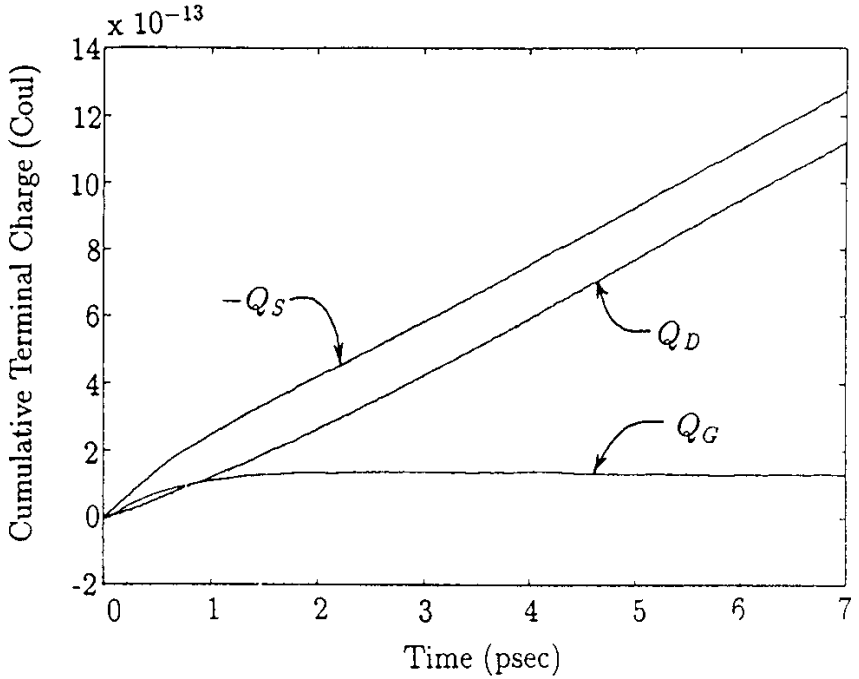


Fig. 2. Cumulative terminal charge vs time for the source, drain and gate terminals for a step change $\Delta V_G = 0.3$ V from $V_G = 0.2$ V. Drain voltage is kept constant at $V_D = 2$ V. Gate length for this device is 0.3 $\mu$m.

- **The cumulative charge contains a steady-state contribution that can be extrapolated and subtracted, to obtain a transient contribution.**

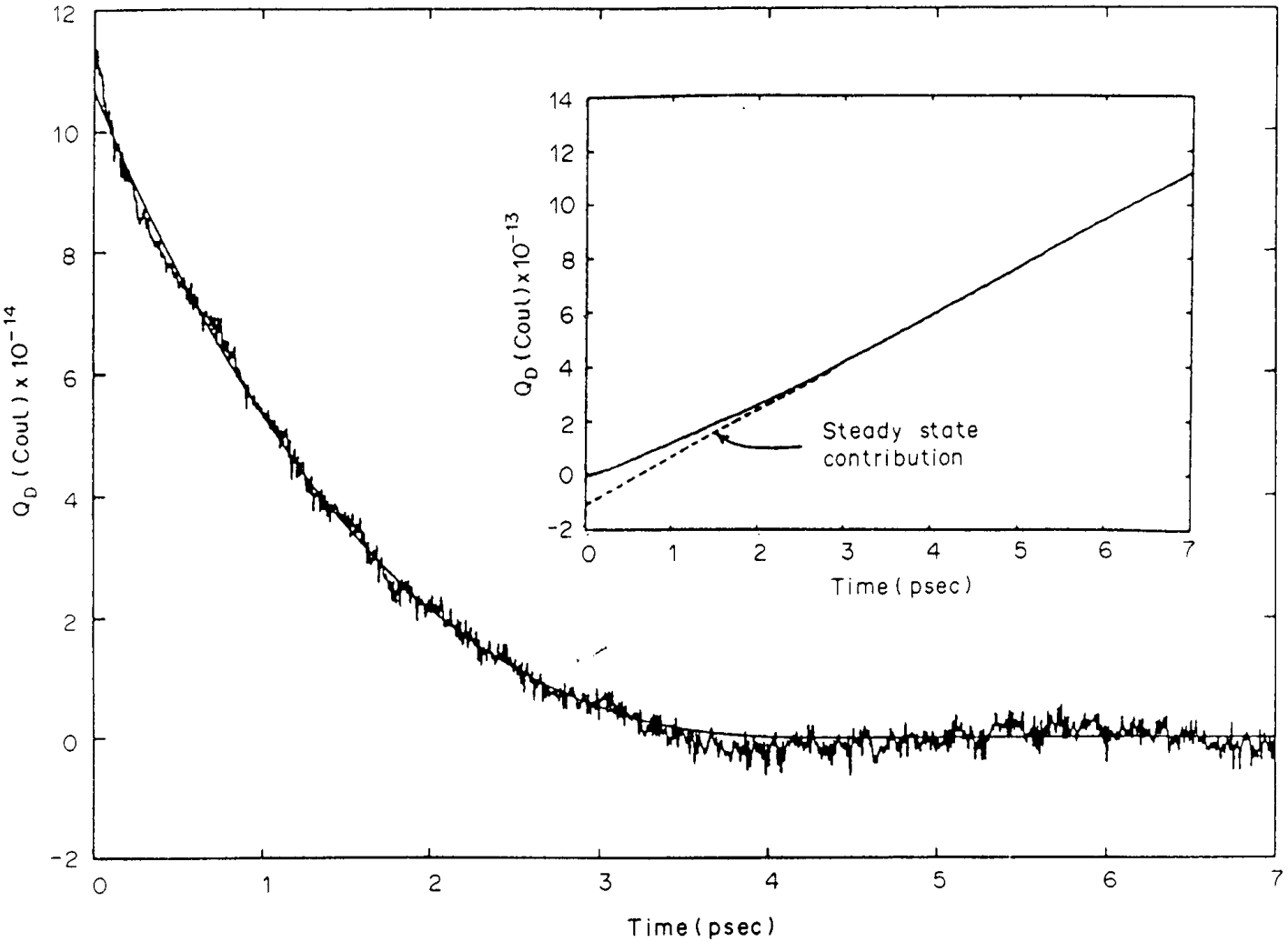


Fig. 3. Cumulative drain charge $Q_D$ vs time after subtracting the steady state contribution. The $Q$-axis has been shifted to make the steady state charge equal to zero. The polynomial approximation is depicted by the smooth curve. The original $Q_D$ vs $t$ curve is shown in the inset. Also shown in the inset is the straight line corresponding to the steady state current.

# Cumulative charge decomposition

$$Q_{ss}(t) = a_{1,ss}\, t + a_{0,ss} \qquad t_{ss} < t < t_{total}$$

$$Q_{tr}(t) = \sum_{n=0}^{N} a_{n,tr}\, t^n$$

- The fitting coefficients are found from

$$I(t) = \frac{dQ}{dt} \quad \text{and} \quad \frac{dI(t)}{dt} = \frac{d^2Q}{dt^2}$$

imposing

$$\frac{dQ_{tr}}{dt} = \frac{dQ_{ss}}{dt}; \qquad \frac{d^2Q_{tr}}{dt^2} = \frac{d^2Q_{ss}}{dt^2} \qquad t = t_{ss}$$

(Patil and Ravaioli, Solid-State Electronics,1991)

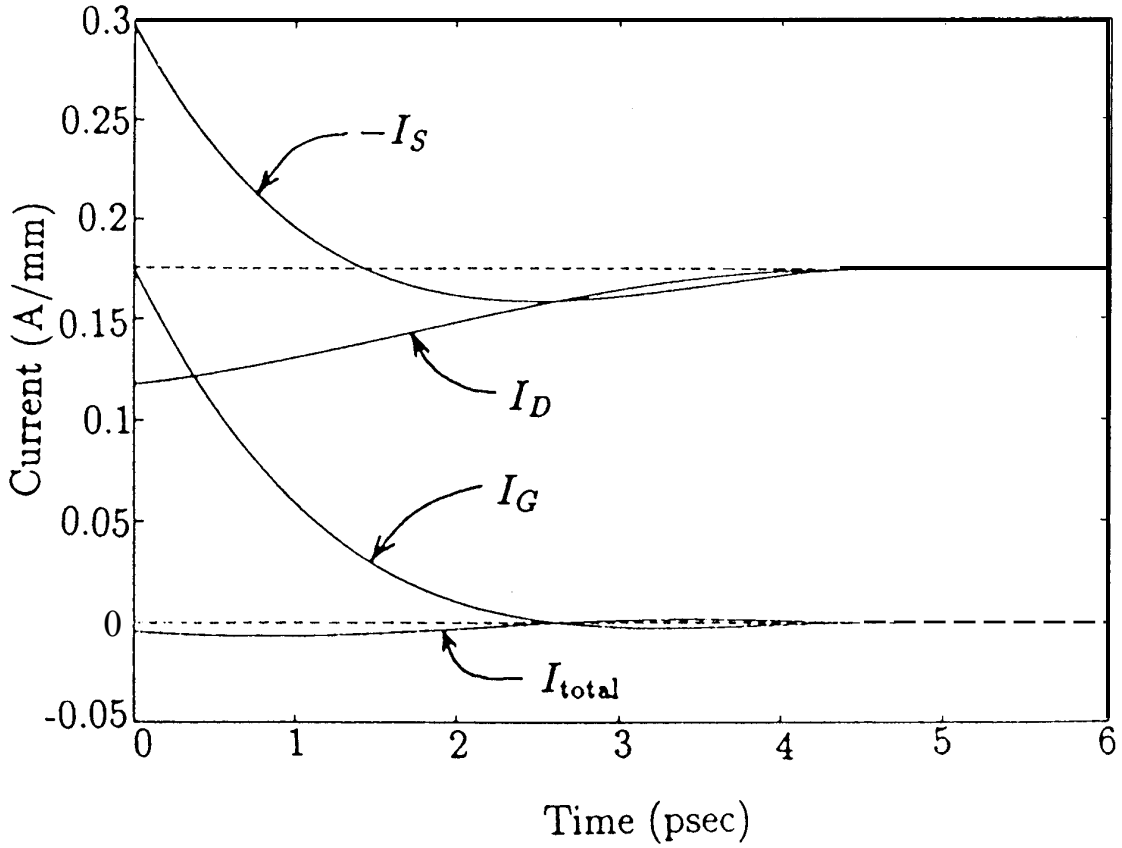


Fig. 4. Terminal currents as a function of time computed from the $Q$ vs $t$ curves of Fig. 2. Currents are defined to be positive if entering a terminal. Also shown is the total current which is close to zero. Dashed lines indicate the steady-state currents. Note that $I_G$ attains its steady-state value about 1 ps before $I_S$ and $I_D$.

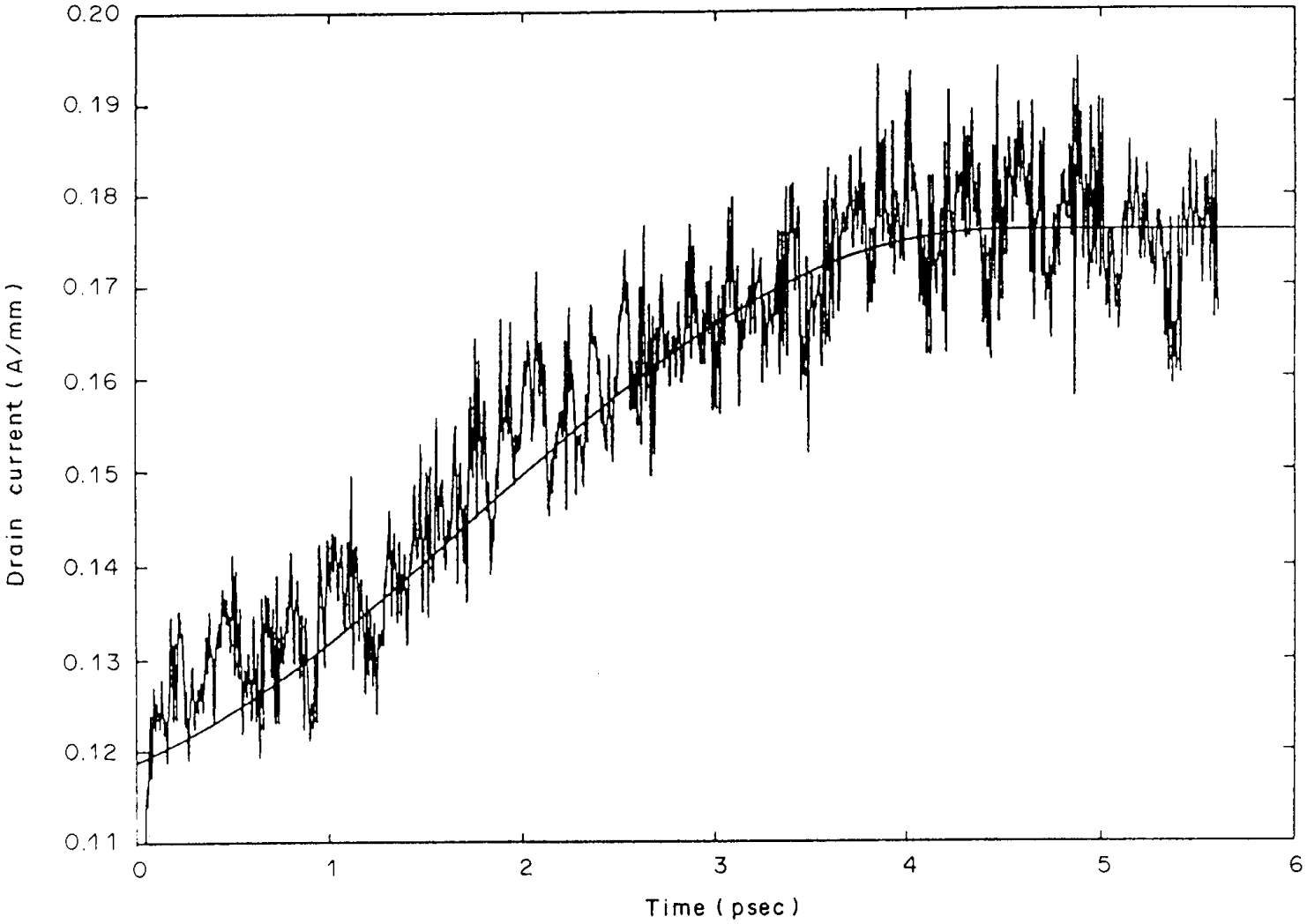


Fig. 5. Raw data for drain current obtained from MC simulation, after averaging for 200 iterations. Each iteration corresponds to 2 fs. The data are for the conditions of Fig. 2. Transient current plotted in Fig. 4 is also reproduced for comparison (smooth curve).

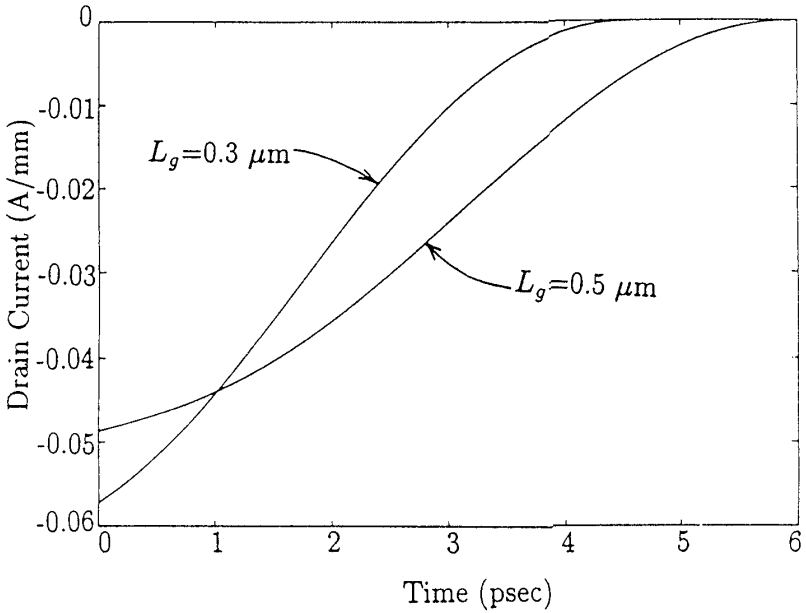


Fig. 6. Drain current transients for two different gate lengths, all other device parameters being the same. $\Delta V_G = 0.3$ V in both cases. The drain voltage is fixed at $V_D = 2$ V. The steady state current is taken as reference.

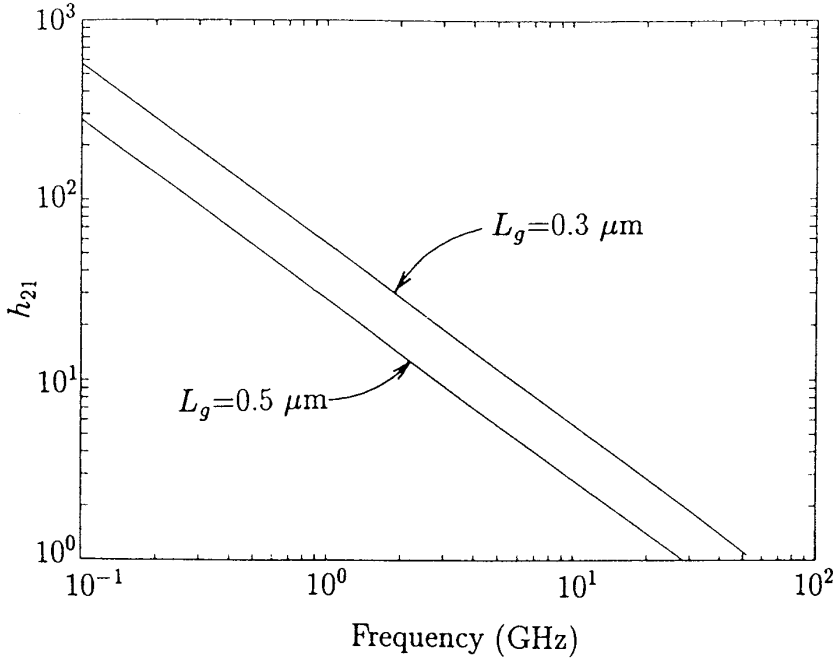


Fig. 7. Current gain $h_{21}$ as a function of frequency for two different gate lengths. The bias conditions are $V_D = 2$ V and $V_G = 0.2$ V.

# Time dependent noise analysis

- **Prerequisite of noise analysis is to obtain accurate values of the instantaneous currents at the terminals, including the displacement contributions.**

- **For a simple quasi-2-D MESFET contact configuration (side contacts), it is possible to formulate an accurate current evaluation (Gruzinskis, Kersulis, Reklaitis, 1991).**

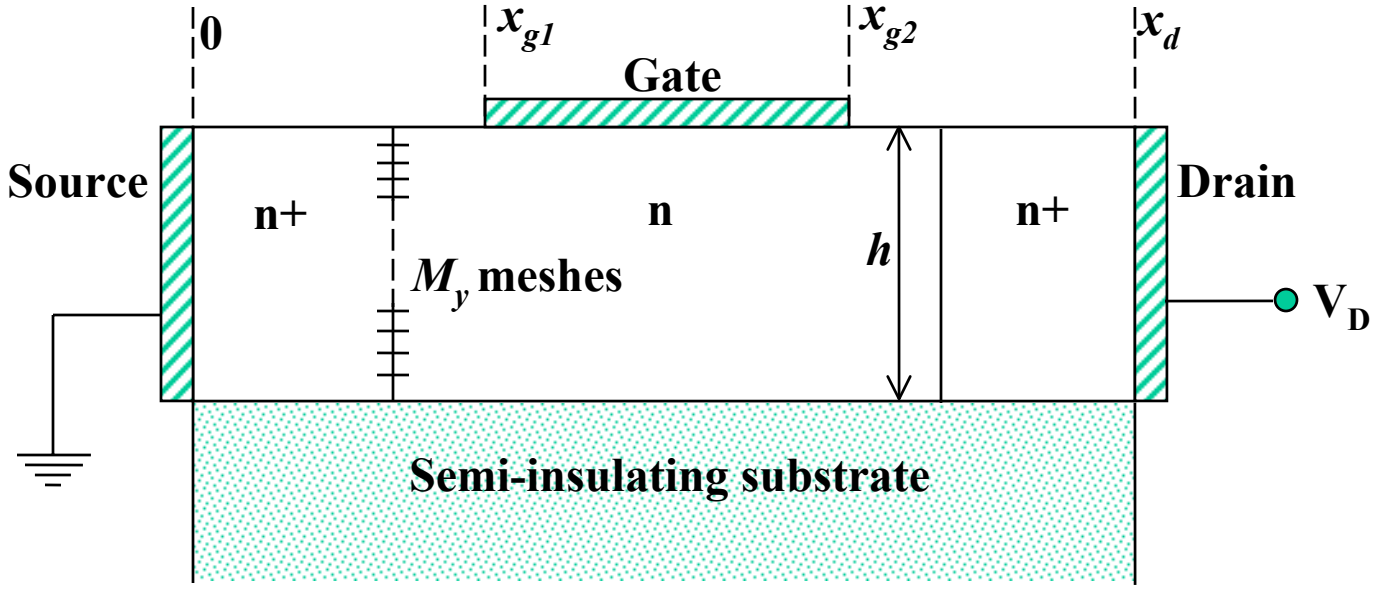

# Terminal Currents – Source

$$I_s(t) = \frac{1}{x_{g1}} \left[ Q \sum_{i}^{\{0 \to x_{g1}\}} v_{xi}(t) - \frac{\varepsilon}{\Delta t} \sum_{j=1}^{M_y} \Delta y_j \left( \varphi(x_{g1}, y_j, t) - \varphi(x_{g1}, y_j, t - \Delta t) \right) \right]$$

$$V_s = 0 \quad \text{(ground)}$$

**$Q$ represents the linear charge density associated to a simulated particle (a rod of charge in the direction perpendicular to the simulation domain).**

## Terminal Currents – Drain

$$I_d(t) = \frac{1}{(x_d - x_{g2})}\left[ Q \sum_{i}^{\{x_{g2} \to x_d\}} v_{xi}(t) \right.$$

$$- \frac{\varepsilon}{\Delta t} \sum_{j=1}^{M_y} \Delta y_j \left( \varphi(x_{g2}, y_j, t) - \varphi(x_{g2}, y_j, t - \Delta t) \right)$$

$$\left. - \frac{\varepsilon h}{\Delta t} \left( V_d(t) - V_d(t - \Delta t) \right) \right]$$

## Terminal Currents – Gate

$$I_g(t) = I_s(t) - I_d(t)$$

# Current-Noise operation

- **The gate and drain voltages remain constant in time, and the fluctuations of the short-circuit currents and their correlations are investigated. The current-noise sources are represented as two correlated current generators at input and output of the device. Since the drain voltage is constant, the last two terms in the drain current equation, cancel each other.**

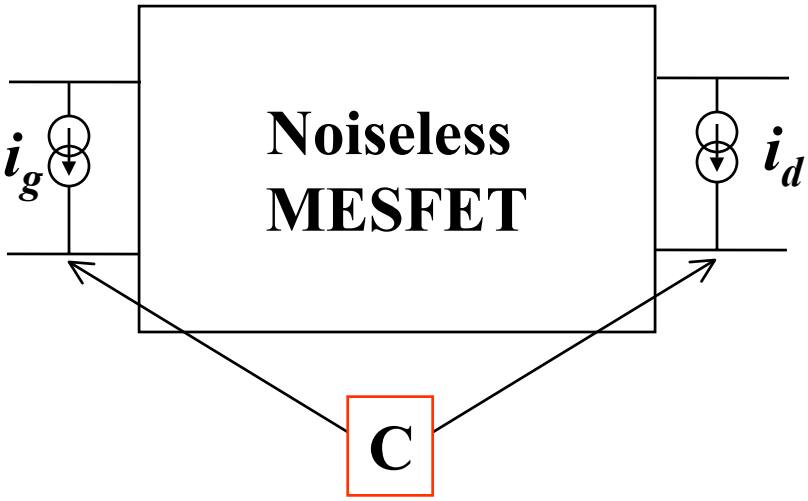

# Voltage-Noise operation

- **The gate voltage and the drain current remain constant in time and the fluctuations of the short-circuit gate current and open circuit drain voltage and their correlation are investigated. The noise sources are represented as correlated current generator in parallel at input and voltage generator in series at the output.**

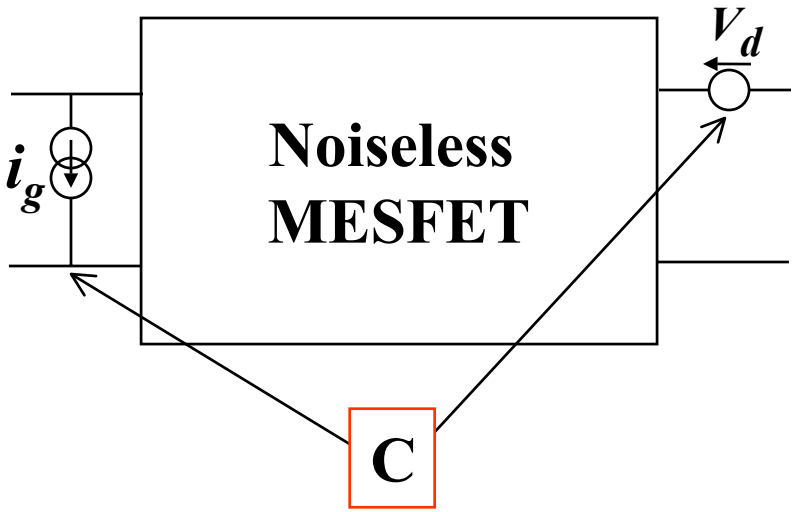

# Voltage-Noise operation

- If we consider a constant drain current $I_{do}$ the instantaneous drain voltage is

$$V_d(t) = V_d(t-\Delta t) - \frac{\Delta t}{\varepsilon h}\left( I_{d0}(x_d - x_{g2}) - Q \sum_{i}^{\{x_{g2}\to x_d\}} v_{xi}(t) \right)$$

$$+ \frac{1}{h}\sum_{j=1}^{M_y} \Delta y_j \left( \varphi(x_{g2}, y_j, t) - \varphi(x_{g2}, y_j, t-\Delta t) \right)$$

- This voltage is evaluated by applying an iterative technique. Poisson equation is repeated at the end of each step: first with the old value of $V_d$ and the new carrier space-distribution, and then with the value of $V_d$ update as above by using the values of $\varphi$ from the preceding solution.

# Transient electromagnetic effects - Maxwell's equations

$$\nabla \times \vec{E}(t) = -\frac{\partial \vec{B}(t)}{\partial t}$$

$$\nabla \times \vec{H}(t) = \frac{\partial \vec{D}(t)}{\partial t} + \vec{J}$$

$$\nabla \cdot \vec{D}(t) = \rho$$

$$\nabla \cdot \vec{B}(t) = 0$$

$$\vec{D}(t) = \varepsilon \vec{E}(t)$$

$$\vec{B}(t) = \mu \vec{H}(t)$$

$$\vec{B} = \nabla \times \vec{A}$$

$$\vec{E} = -\frac{\partial \vec{A}}{\partial t} - \nabla \times \phi$$

$$\nabla \cdot \vec{A} = -\mu\varepsilon \frac{\partial \phi}{\partial t}$$

$$\nabla \times \nabla \times \vec{A} = \nabla \nabla \cdot \vec{A} - \nabla^2 \vec{A} = \mu \vec{J} = \varepsilon\mu \frac{\partial^2 \vec{A}}{\partial t^2} - \varepsilon \nabla \frac{\partial \vec{A}}{\partial t}$$

# Wave equations

$$\Rightarrow \quad \boxed{\nabla^2 \vec{A} - \varepsilon\mu \frac{\partial^2 \vec{A}}{\partial t^2} = -\mu \vec{J}}$$

$$-\nabla^2 \phi - \frac{\partial}{\partial t} \nabla \cdot \vec{A} = -\frac{\rho}{\varepsilon}$$

$$\Rightarrow \quad \boxed{\nabla^2 \phi - \varepsilon\mu \frac{\partial^2 \phi}{\partial t^2} = -\frac{\rho}{\varepsilon}}$$

- **Instead of Poisson equation, one should solve the retarded potential wave equation, with time-dependent voltage boundary conditions.**

# When is full wave analysis necessary?

- **Example: GaAs**

$$\varepsilon = 12.9\varepsilon_0 \qquad \mu = \mu_o \qquad n_i(T = 300K) = 1.76\times 10^6\ \text{cm}^{-3}$$

$$\mu_n = 8500\ \text{cm}^2/V-s \qquad \mu_p = 400\ \text{cm}^2/V-s$$

$$f = 1.0\ \ \text{THz} \quad \Rightarrow \quad \omega\varepsilon = 717.31\ \ \text{S/m}$$

**Perfect dielectric** $\quad \sigma = 0$

$$\lambda = \frac{c}{\sqrt{\varepsilon_r}\, f} \approx 83.5\ \ \mu\text{m}$$

**Intrinsic GaAs** $\quad \sigma = qn_i\left(\mu_n + \mu_p\right) \approx 2.55\times 10^{-7}\ \ \text{S/m}$

$$\sigma \ll \omega\varepsilon \quad \Rightarrow \lambda \approx 83.5\ \ \mu\text{m}$$

**imperfect dielectric**

## When is full wave analysis necessary?

- **n-type GaAs** $\sigma \approx q\mu_n n$

$$\lambda = \frac{\sqrt{2}}{f\sqrt{\mu_o \varepsilon}}\left(\sqrt{1+\left(\frac{\sigma}{\omega\varepsilon}\right)^2}+1\right)^{-1/1}$$

- **Worst case analysis: assume in all cases the mobility for undoped material. Actual wavelength will be somewhat longer than below.**

| $n$ | $\sigma$ | $\lambda$ |
|---|---|---|
| $10^{15}$ cm$^{-3}$ | $1.36\times10^{2}$ S/m | 83.1 μm |
| $10^{16}$ cm$^{-3}$ | $1.36\times10^{3}$ S/m | 66.62 μm |
| $10^{17}$ cm$^{-3}$ | $1.36\times10^{4}$ S/m | 26.42 μm |
| $10^{18}$ cm$^{-3}$ | $1.36\times10^{5}$ S/m | 8.55 μm |
| $10^{19}$ cm$^{-3}$ | $1.36\times10^{6}$ S/m | 2.7 μm |

- **Conclusions: In the active regions of microwave and high-speeddevices with moderate dopings, the wavelength is expected to be much larger than the space scale and the electrostatic Poisson equation is adequate.**

- **Modern MESFET structures may have channel concentrations of up to $5\times10^{18}$ cm $^{-3}$. Devices with conduction channels at heterointerfaces may exhibit high concentrations and very high mobilities. Because of the large conductivity, the wavelength may be comparable with the space scale of active regions in certain regimes.**

- **For reference, the walength in copper**

$$\sigma = 5.8\times10^{7}\ \text{S/m} \qquad \varepsilon=\varepsilon_0 \qquad \mu = \mu_o$$

$$f = 1.0\ \text{THz} \quad \Rightarrow \quad \lambda \approx 0.5\ \mu\text{m}$$

## Real Space Transfer Devices

- **The real space transfer effect applies to carriers crossing a heterojunction, after gaining sufficient energy from the field along the interface.**

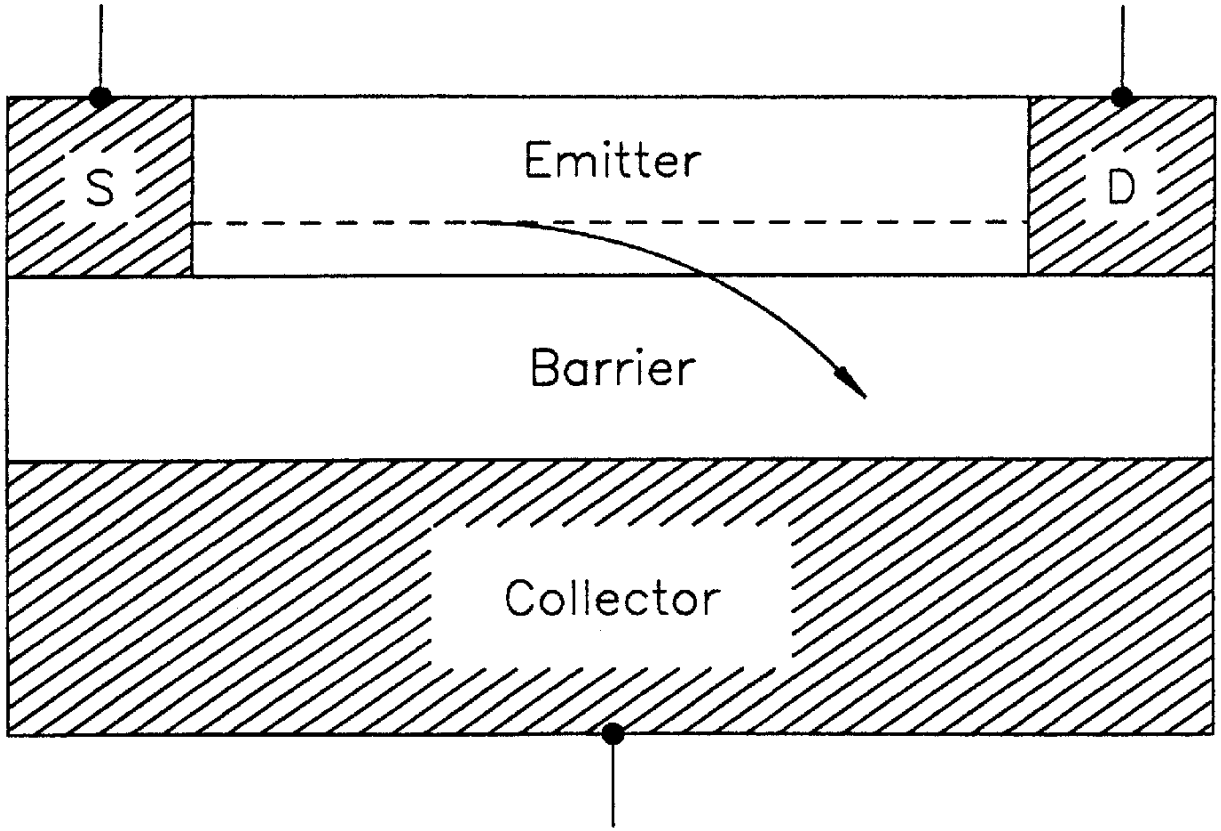

# Collector Up Real Space Transfer Transistor (RSTT)

- **This is similar to a standard MODFET device, with gate biased to attract electrons.**

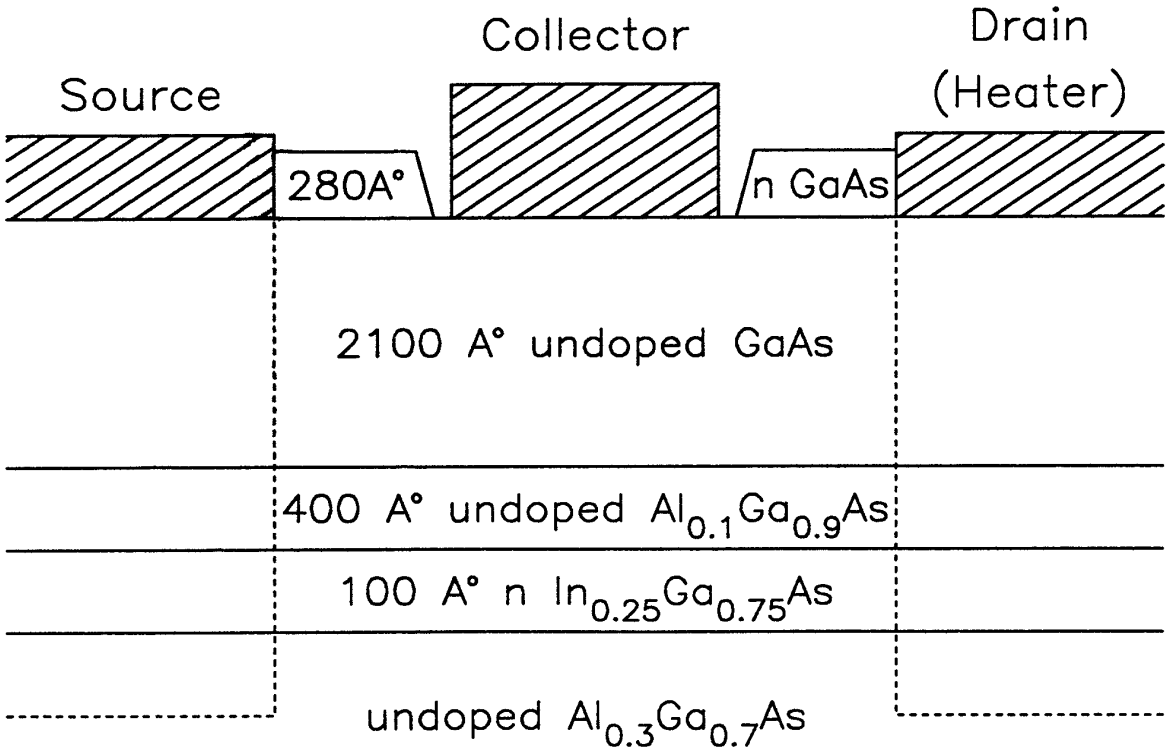

# Simulated RSTT Structure

- **For scaling studies, the length of the gate L is kept equal to its distance from source and heater.**

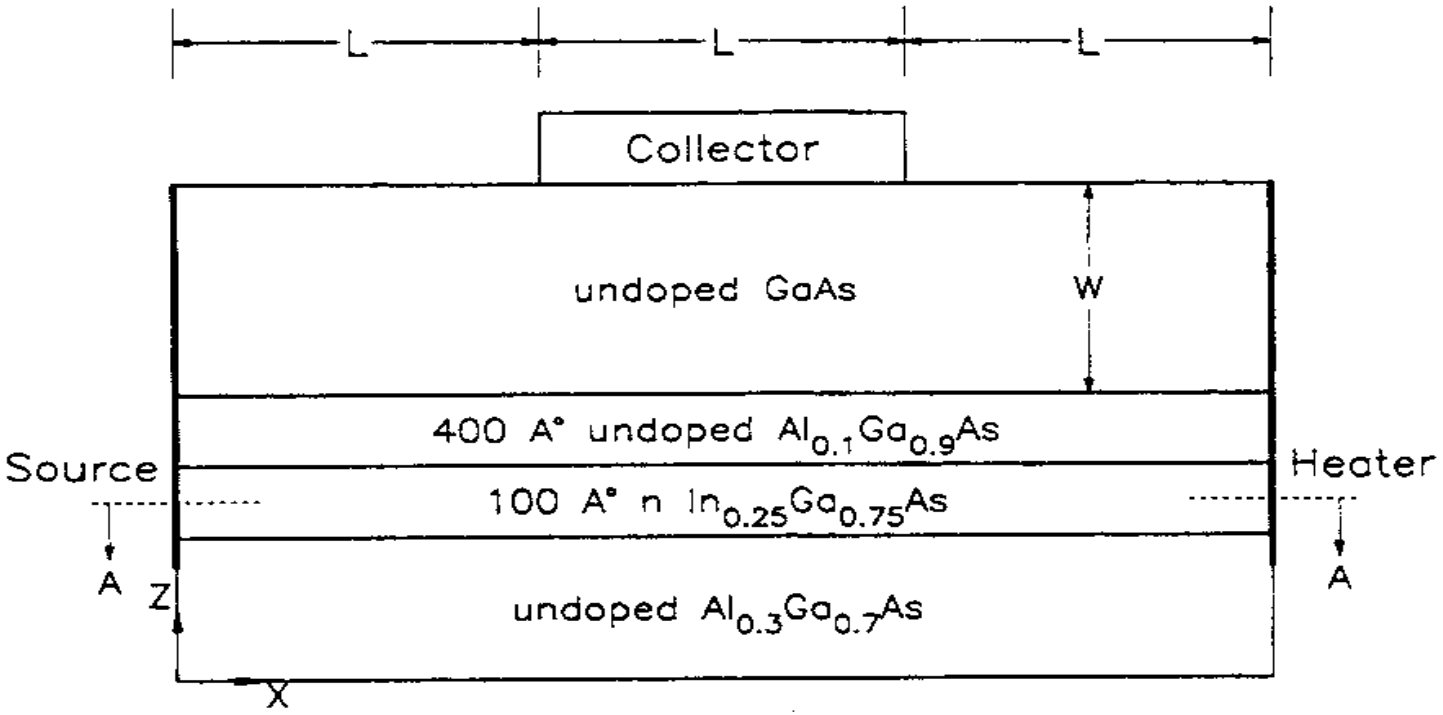

# Details of the Hetero-interface

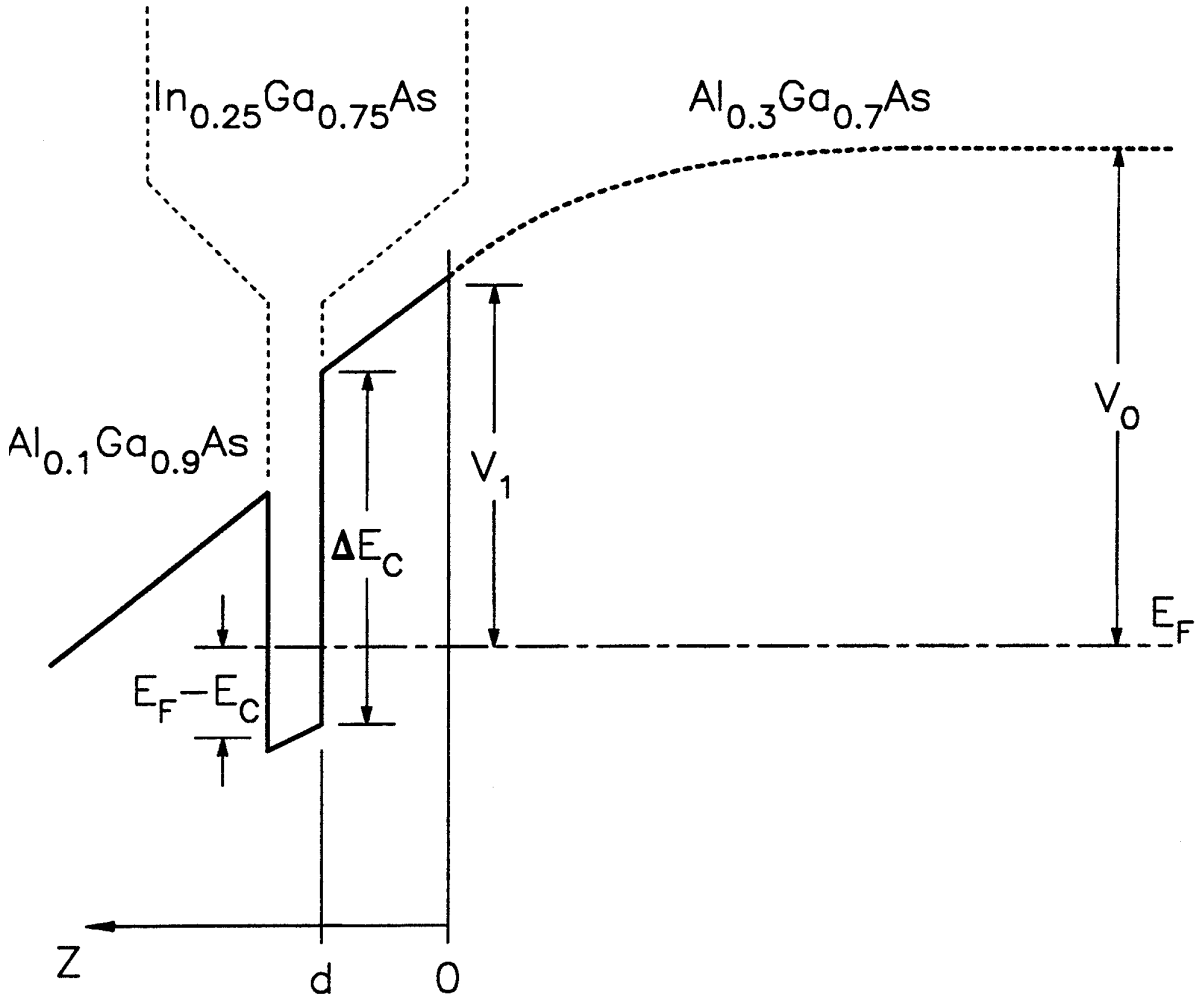

## Experimental curves for a sample RSTT

- **Source current saturates; heater current has slight Negative Differential Resistance (NDR) region; collector current shows large leakage at $V_H = 0$.**

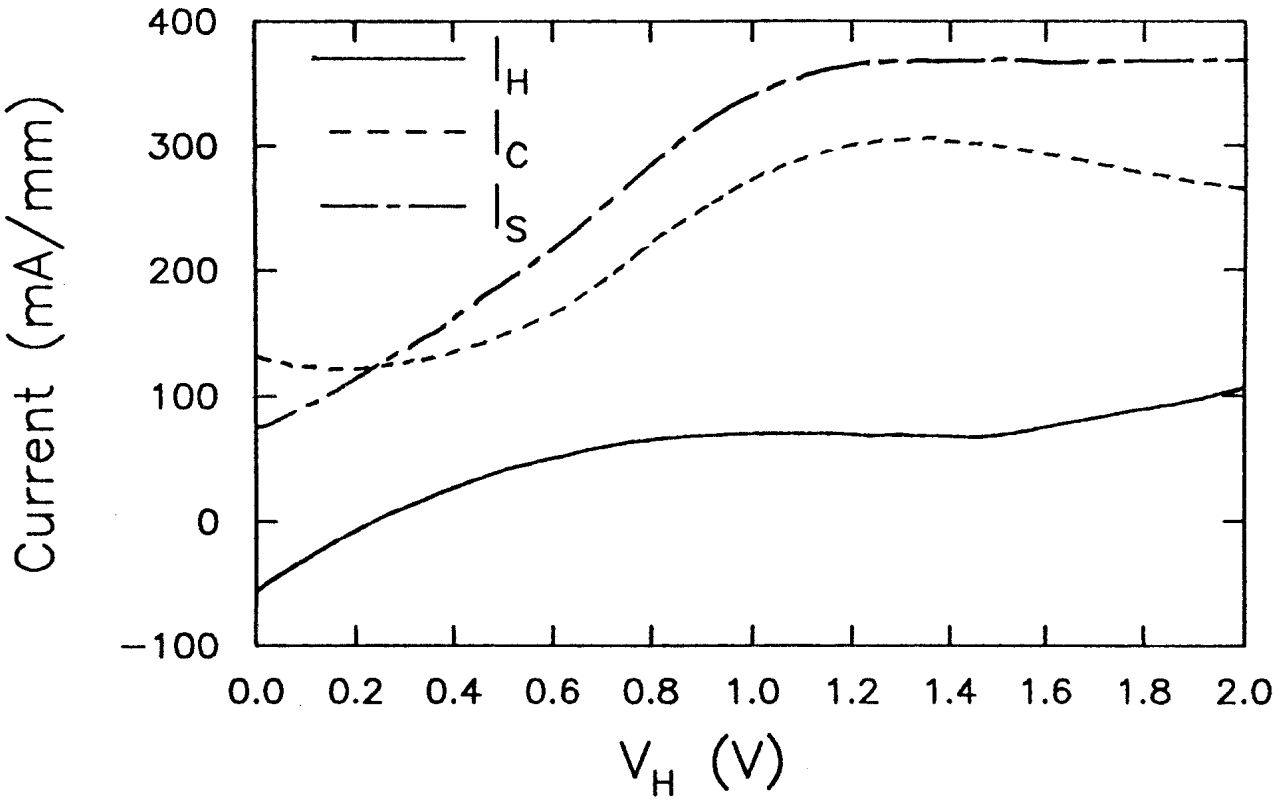

# Monte Carlo simulation results for RSTT

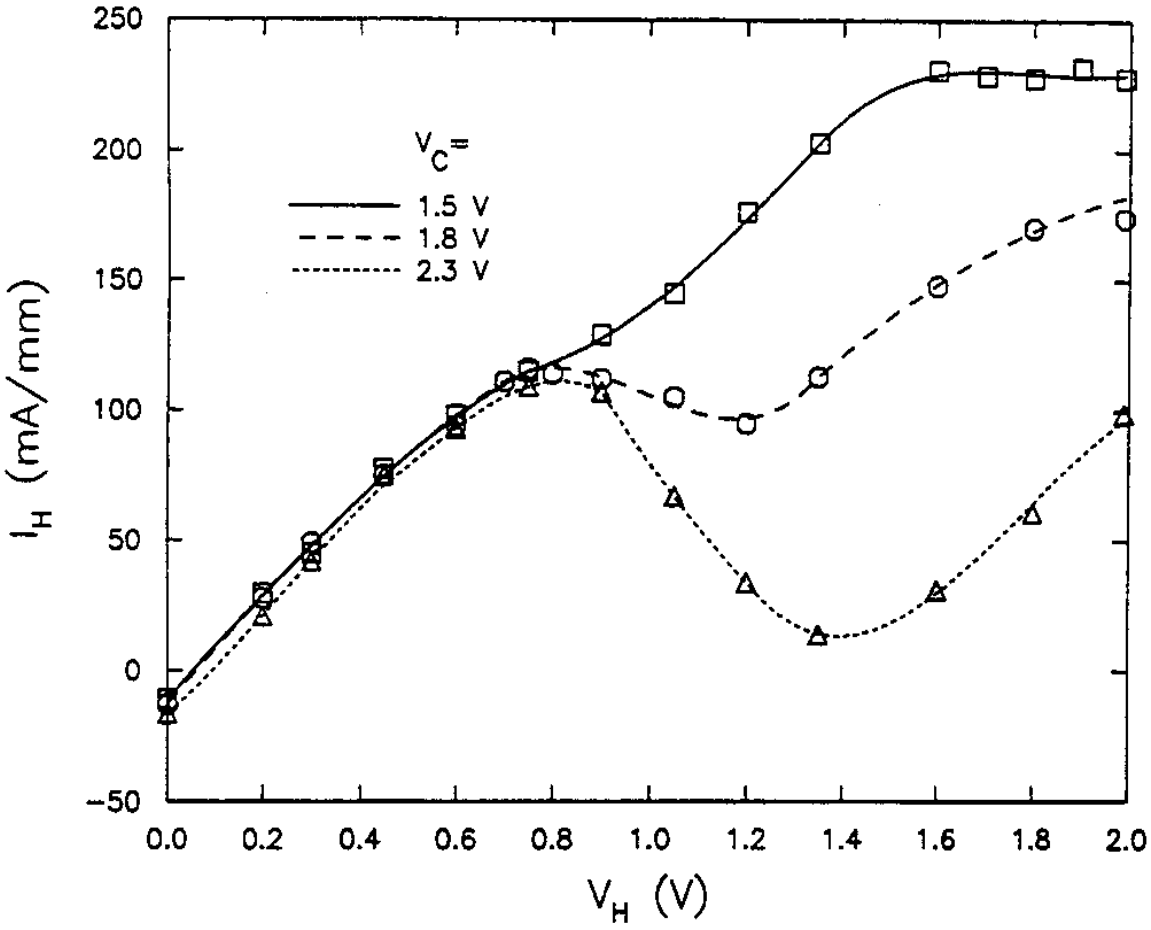


(a)

Fig. 3. Calculated terminal currents versus heater voltage for various values of collector voltage. (a) Heater current. (b) Collector current. (c) Source current. ($L = 1.0\ \mu m$, $W = 0.21\ \mu m$.)

# Monte Carlo simulation results for RSTT

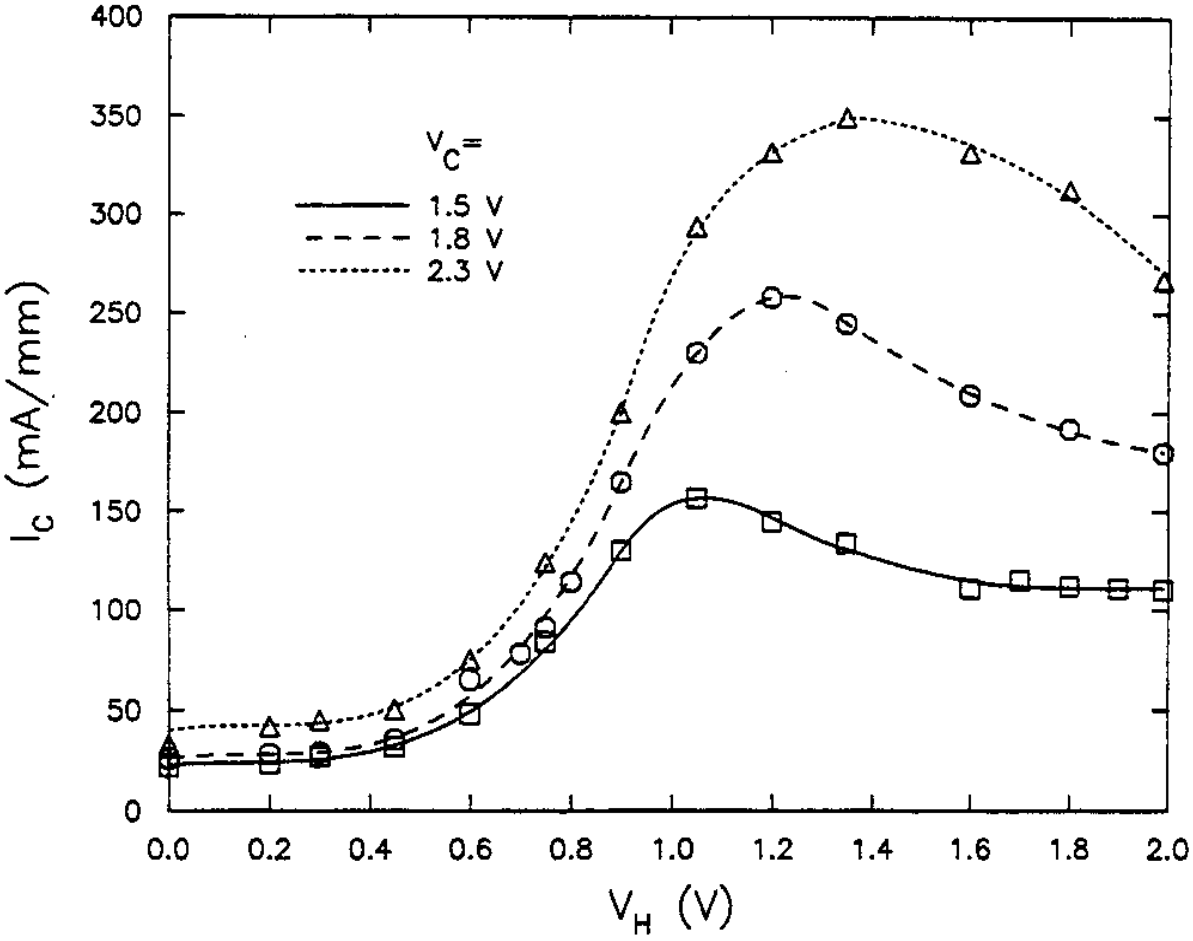


(b)

Fig. 3. Calculated terminal currents versus heater voltage for various values of collector voltage. (a) Heater current. (b) Collector current. (c) Source current. ($L = 1.0\ \mu m$, $W = 0.21\ \mu m$.)

# Monte Carlo simulation results for RSTT

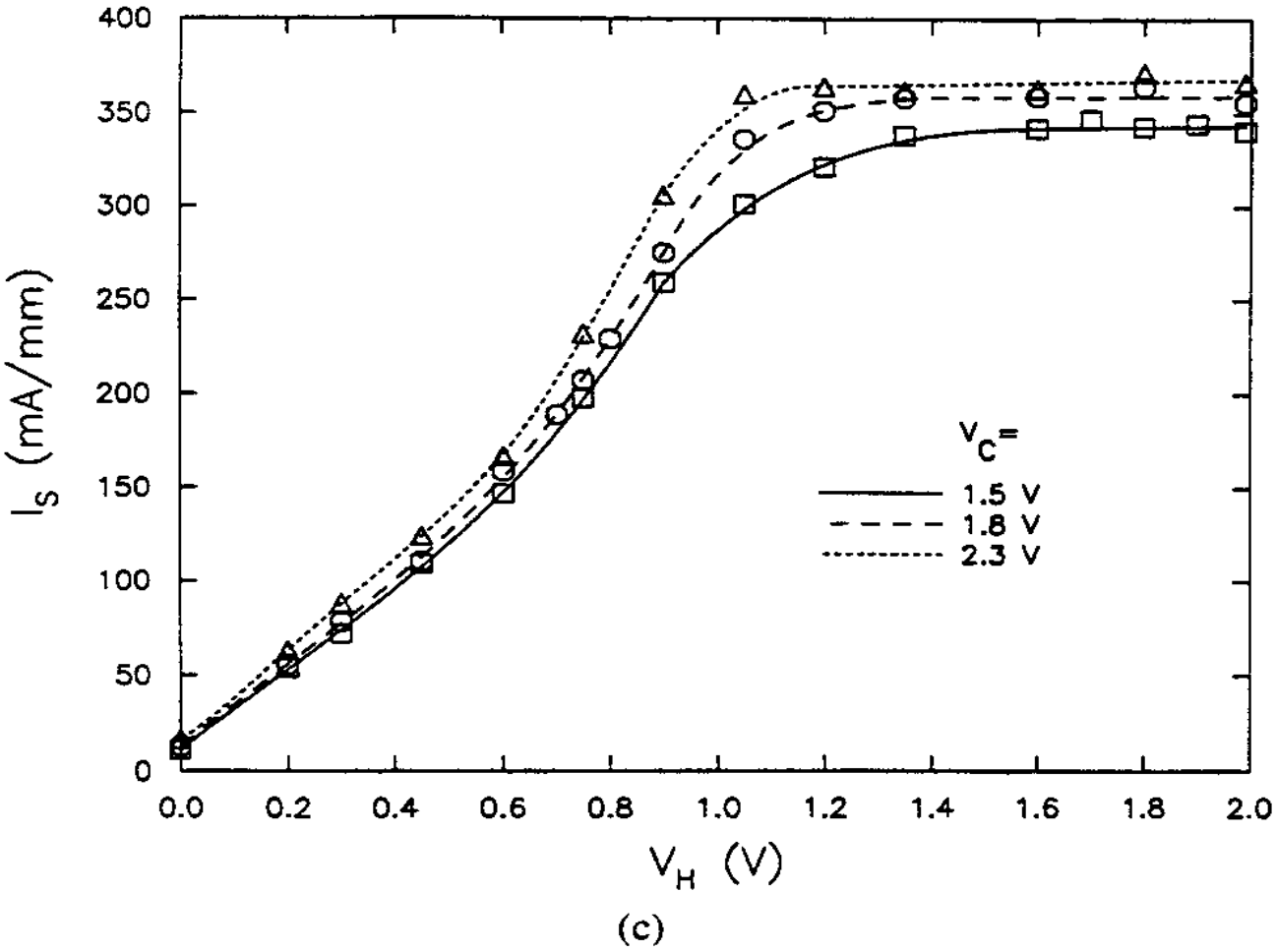


Fig. 3. Calculated terminal currents versus heater voltage for various values of collector voltage. (a) Heater current. (b) Collector current. (c) Source current. ($L = 1.0\ \mu m$, $W = 0.21\ \mu m$.)

# Channel behavior with varying heater voltage

$$(L = 1.0\,\mu\text{m}, \quad W = 0.21\,\mu\text{m}, \quad V_C = 1.8V)$$

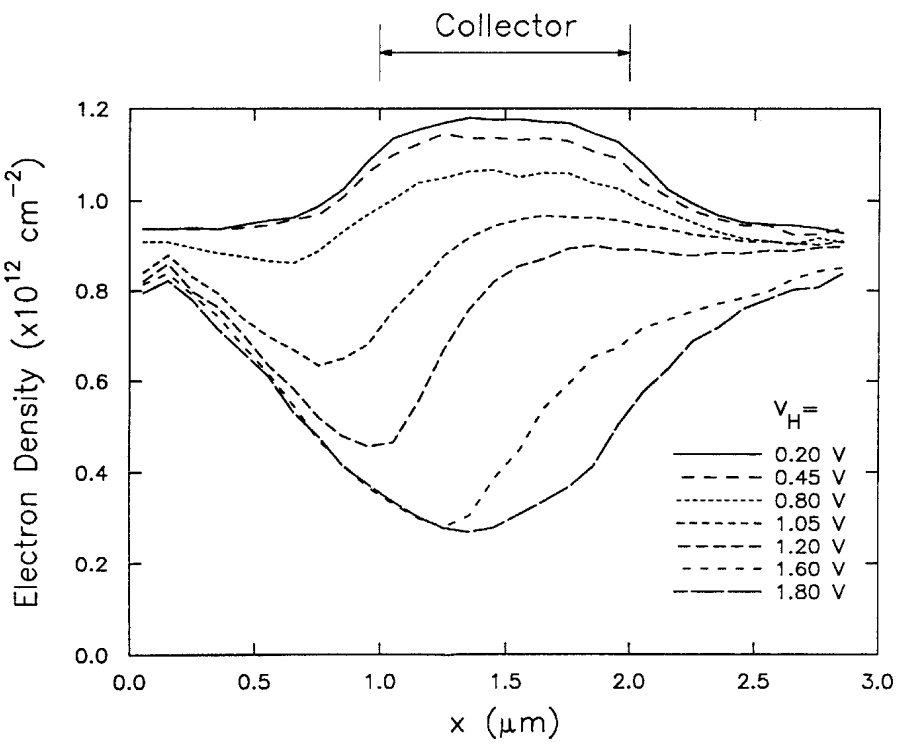


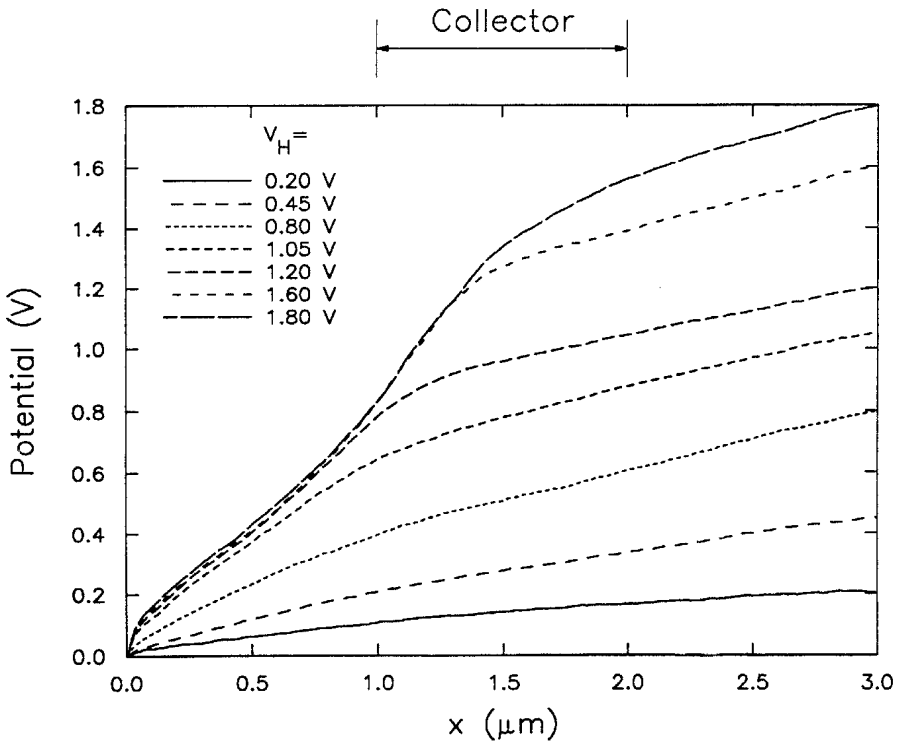

## Net Real Space Transfer rate

$$(L = 1.0\,\mu\text{m}, \quad W = 0.21\,\mu\text{m}, \quad V_C = 1.8V)$$

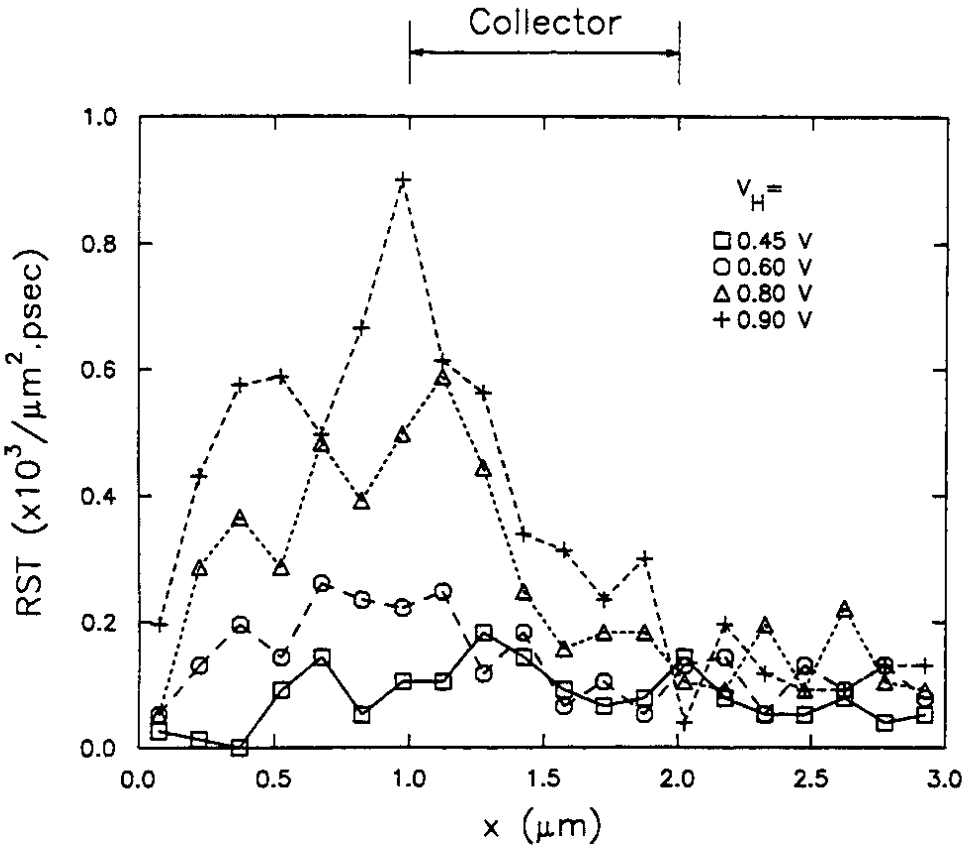


Fig. 6. Rate of *net* real-space transfer from source to heater. $x$ is the distance from the source. ($L$ = 1.0 $\mu$m, $W$ = 0.21 $\mu$m, $V_C$ = 1.8 V.)

# Actual Real Space Transfer from and into channel

$$(L = 1.0\,\mu\text{m}, \quad W = 0.21\,\mu\text{m}, \quad V_H = 1.05V, \quad V_C = 1.8V)$$

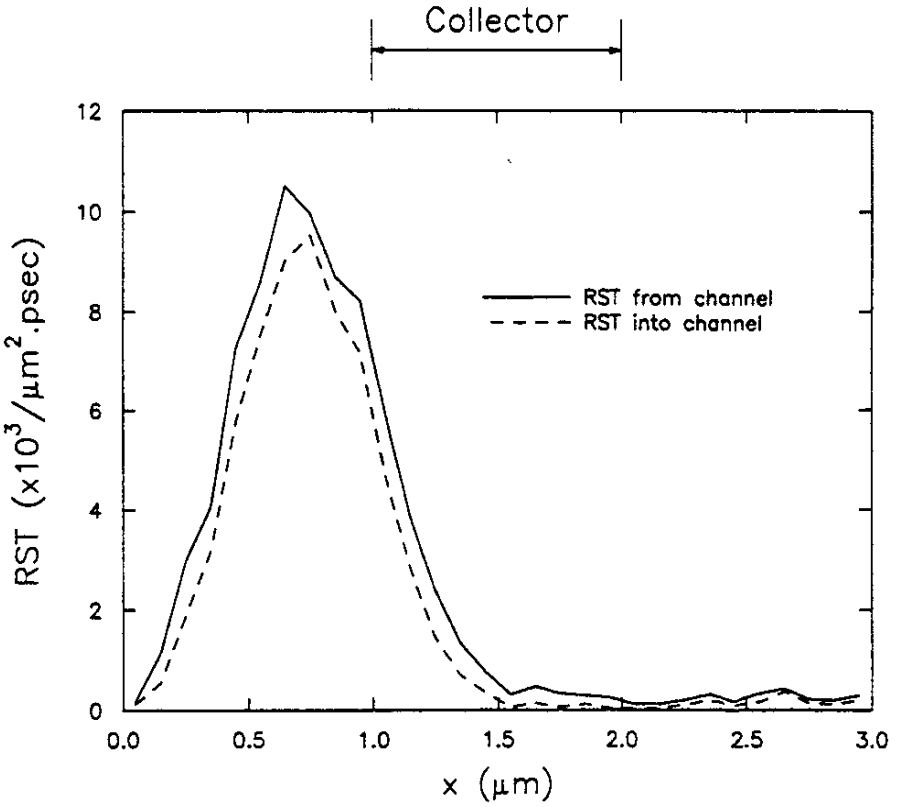


Fig. 7. Rate of real-space transfer from the InGaAs channel to $Al_{0.1}Ga_{0.9}As$ (solid line) and from $Al_{0.1}Ga_{0.9}As$ to the InGaAs channel (dashed line). $x$ is the distance from the source. ($V_H$ = 1.05 V, $V_C$ = 1.8 V, $L$ = 1.0 $\mu$m, $W$ = 0.21 $\mu$m.)

## Total RST scross heterojunction

$$(L = 1.0\ \mu\text{m}, \quad W = 0.21\ \mu\text{m}, \quad V_C = 1.8V)$$

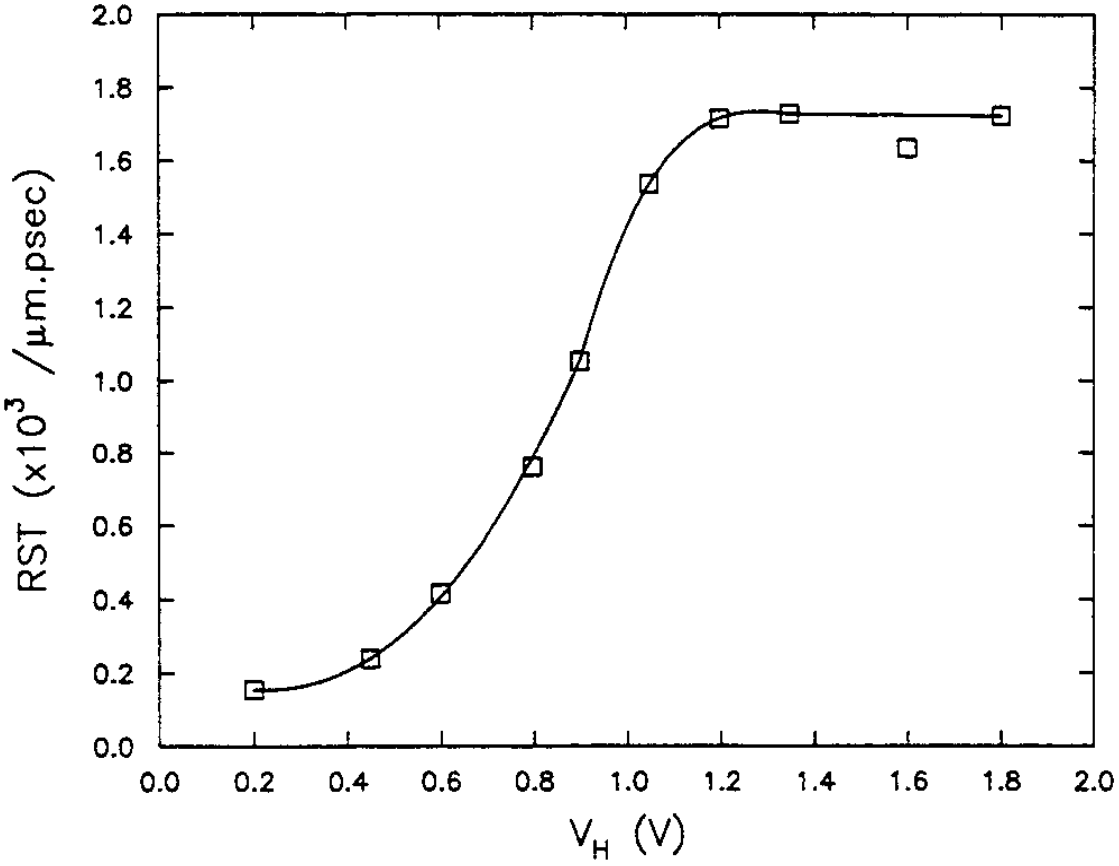


Fig. 8. Total rate of net real-space transfer across the top heterointerface as a function of $V_H$. ($L$ = 1.0 $\mu$m, $W$ = 0.21 $\mu$m, $V_C$ = 1.8 V.)

# Scaling with L

$$(W = 0.21\,\mu\text{m}, \quad V_C = 1.8V)$$

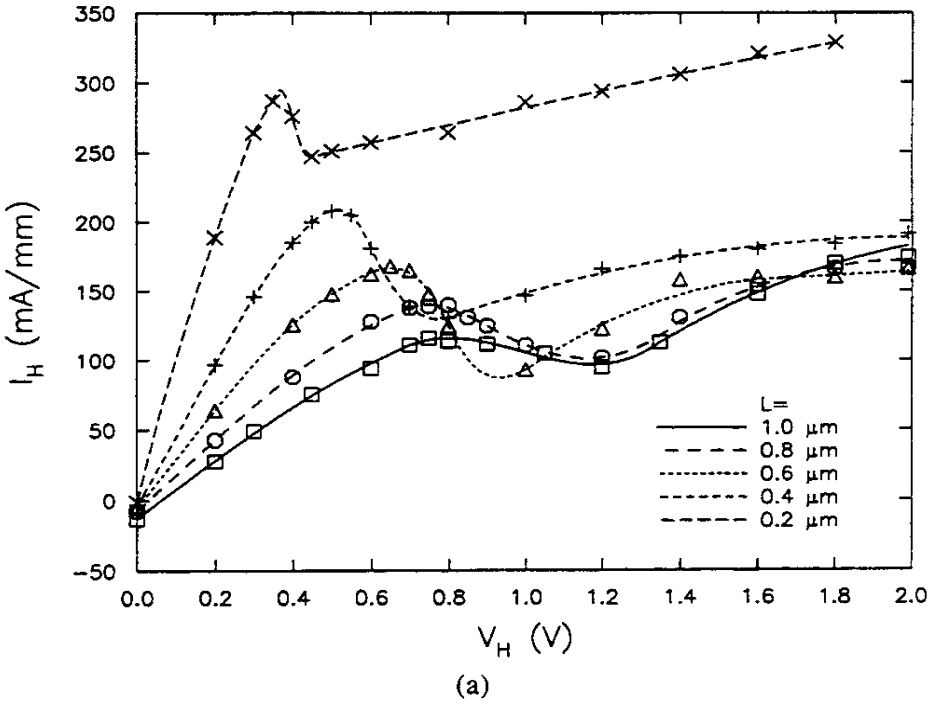


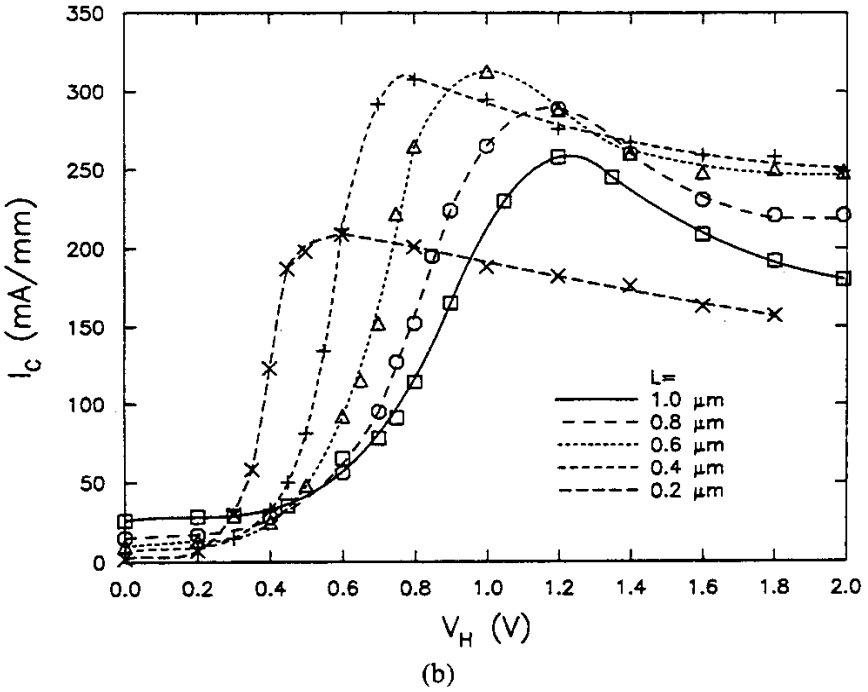


Fig. 9. Calculated terminal currents versus heater voltage for various values of $L$. (a) Heater current. (b) Collector current. ($V_C$ = 1.8 V, $W$ = 0.21 $\mu$m.)

# Scaling with W

$$(L = 0.4\,\mu\text{m}, \quad V_C = 1.8V)$$

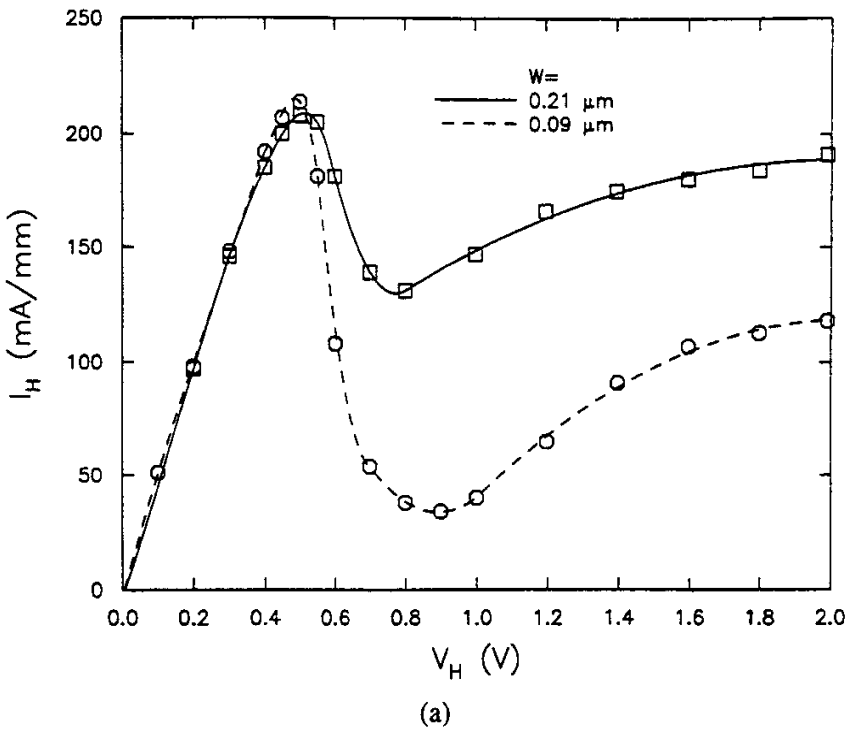


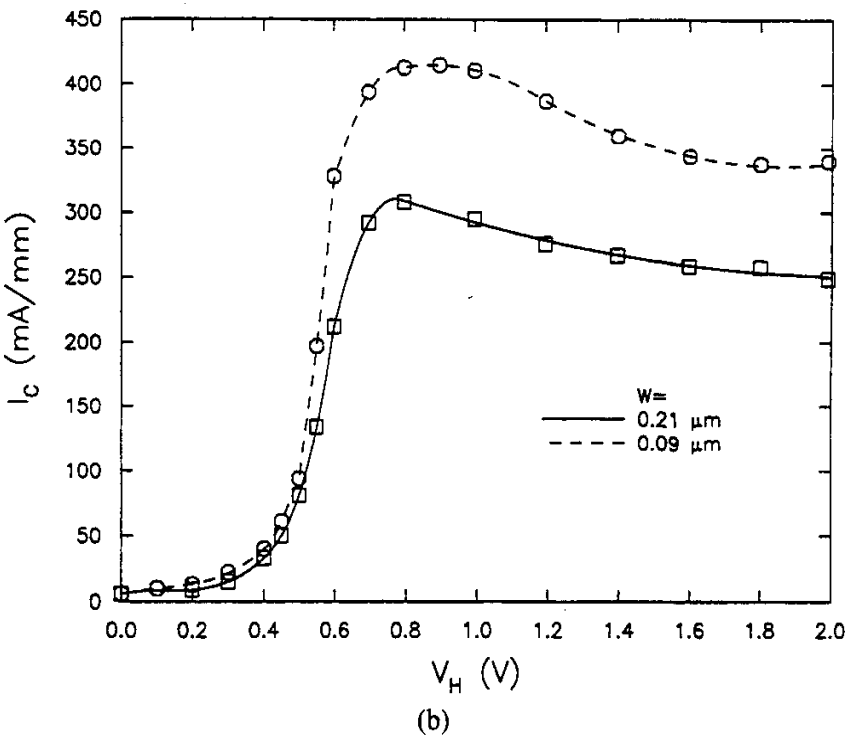


Fig. 10. Calculated terminal currents versus heater voltage for two values of $W$. (a) Heater current. (b) Collector current. ($V_C$ = 1.8 V, $L$ = 0.4 $\mu$m.)

# Collector current transient

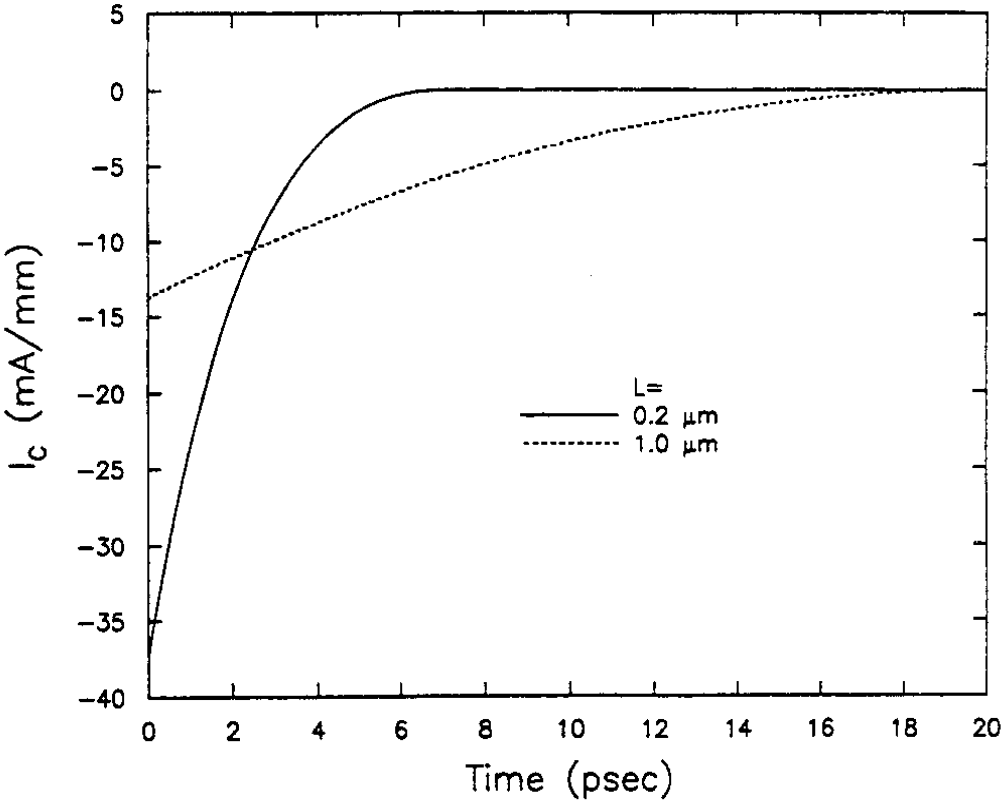


Fig. 11. Collector current versus time due to a step change $\Delta V_H = 50$ mV for two different values of $L$. The steady-state current is taken as a reference. ($V_C = 1.8$ V, $W = 0.21$ μm.)

**Video animation: switching of RSTT simulated with Monte Carlo**